© 2014. Published by The Company of Biologists Ltd | Development (2014) 141, 3848-3858 doi:10.1242/dev.105981

RESEARCH ARTICLE

STEM CELLS AND REGENERATION

Small molecule-directed specification of sclerotome-like chondroprogenitors and induction of a somitic chondrogenesis program from embryonic stem cells

Jiangang Zhao[1,*], Songhui Li[2,‡], Suprita Trilok[1], Makoto Tanaka[2,¶], Vanta Jokubaitis-Jameson[2,§], Bei Wang[2,‡], Hitoshi Niwa[3] and Naoki Nakayama[1,2,4,]**

ABSTRACT

Pluripotent embryonic stem cells (ESCs) generate rostral paraxial mesoderm-like progeny in 5-6 days of differentiation induced by Wnt3a and Noggin (Nog). We report that canonical Wnt signaling introduced either by forced expression of activated β-catenin, or the small-molecule inhibitor of Gsk3, CHIR99021, satisfied the need for Wnt3a signaling, and that the small-molecule inhibitor of BMP type I receptors, LDN193189, was able to replace Nog. Mesodermal progeny generated using such small molecules were chondrogenic *in vitro*, and expressed trunk paraxial mesoderm markers such as Tcf15 and Meox1, and somite markers such as Uncx, but failed to express sclerotome markers such as Pax1. Induction of the osteochondrogenically committed sclerotome from somite requires sonic hedgehog and Nog. Consistently, Pax1 and Bapx1 expression was induced when the isolated paraxial mesodermal progeny were treated with SAG1 (a hedgehog receptor agonist) and LDN193189, then Sox9 expression was induced, leading to cartilaginous nodules and particles in the presence of BMP, indicative of chondrogenesis via sclerotome specification. By contrast, treatment with TGFβ also supported chondrogenesis and stimulated Sox9 expression, but failed to induce the expression of Pax1 and Bapx1. On ectopic transplantation to immunocompromised mice, the cartilage particles developed under either condition became similarly mineralized and formed pieces of bone with marrow. Thus, the use of small molecules led to the effective generation from ESCs of paraxial mesodermal progeny, and to their further differentiation *in vitro* through sclerotome specification into growth plate-like chondrocytes, a mechanism resembling *in vivo* somitic chondrogenesis that is not recapitulated with TGFβ.

KEY WORDS: Pluripotent stem cells, Paraxial mesoderm, Sclerotome, Chondrogenesis, Mouse

INTRODUCTION

Repair of large bone defects and damaged cartilage remain a significant clinical challenge. The combination of therapy with mesenchymal stromal cells (MSCs) and the use of biodegradable biomimetic scaffolds appears to be a promising therapeutic approach, as MSCs from bone marrow or fat tissue can be both osteogenic and chondrogenic under certain conditions *in vitro* and *in vivo*. However, the difficulty of the approach lies in controlling the clinical outcome. As bone and cartilage are naturally formed during embryogenesis, we hypothesize that one way to alleviate the difficulty is to use embryonic osteochondro-progenitors instead of adult cells.

For human embryonic cells, pluripotent stem cells (PSCs) [i.e. embryonic stem cells (ESCs) or induced pluripotent stem cells (iPSCs)] are thus far the only practical source. PSC culture is scalable, and *in vitro* differentiation of PSCs can mimic early embryogenesis (Murry and Keller, 2008; Nishikawa et al., 2007) such that large numbers of a particular type of embryonic cell can be obtained under the appropriate conditions of differentiation to mimic embryogenesis. Furthermore, the wealth of information emanating from developmental biology studies is expected to aid in the discovery and refinement of such conditions. However, although ESCs have been shown to generate mesenchymal progeny capable of developing cartilage *in vitro* (Nakayama and Umeda, 2011), the resultant chondrogenic activities were generally poor, and with the exception of ours and a few others (Craft et al., 2013; Oldershaw et al., 2010; Tanaka et al., 2009; Umeda et al., 2012), most reports did not define the developmental origin of the mesenchymal cells generated. The osteochondro-progenitors that develop during embryogenesis are limb bud mesenchyme (derived from lateral plate mesoderm) responsible for limb bone and cartilage generation, sclerotome (from somite/rostral paraxial mesoderm) responsible for rib, vertebral joint, intervertebral disc and vertebral body formation, and ectomesenchyme (from cranial neural crest) responsible for craniofacial bone and cartilage generation. These progenitors are differentially specified through the action of protein factors such as Wnt, and members of the transforming growth factor (TGF)β-superfamily: Nodal and bone morphogenetic protein (BMP), and their inhibitors. Therefore, to make use of such knowledge to improve and refine the condition for osteochondro-progenitor development, PSC differentiation should be directed toward a particular lineage.

In the first step toward testing our hypothesis, we have previously demonstrated that somitic/rostral presomitic mesoderm-like progeny (hereafter referred to as 'rostral paraxial mesoderm') is specified from mouse and human ESCs and is enriched in the Flk1(Kdr)$^{-}$Pdgfrα^{+} cell fraction of embryoid bodies (EBs) generated in a chemically defined medium (CDM) (Tanaka et al., 2009; Umeda et al., 2012). The specification process is strictly dependent on the activation of Wnt signaling and suppression of BMP signaling (Craft et al., 2013; Tanaka et al., 2009; Umeda et al., 2012).

Considering future application to humans, it is important to determine whether the PSC progeny developed *in vitro* behave in the

[1]Institute of Molecular Medicine, The University of Texas Health Science Center Medical School at Houston, Houston, TX 77030, USA. [2]Australian Stem Cell Centre, Monash University, Clayton, Victoria 3800, Australia. [3]RIKEN Center for Developmental Biology, Kobe 650-0047, Japan. [4]Department of Anatomy and Developmental Biology, Monash University, Clayton, Victoria 3800, Australia. *Present address: The University of Texas Medical Branch at Galveston, Galveston, TX 77555, USA. ‡Present address: CSIRO, Clayton, Victoria 3168, Australia. §Present address: The University of Melbourne, Parkville, Victoria 3052, Australia. ¶Present address: Department of Orthopaedic Surgery, Osaka Police Hospital, Osaka 543-0035, Japan.

**Author for correspondence (naoki.nakayama@uth.tmc.edu)

Received 13 November 2013; Accepted 16 August 2014

Development (2014) 141, 3848-3858 doi:10.1242/dev.105981

same way as the *in vivo* progeny and generate mature progeny. Axial skeletogenesis by somite goes through the osteochondrogenically committed progeny, sclerotome (Chal and Pourquié, 2009; Dockter, 2000), in a process involving platelet-derived growth factor (PDGF) (Hoch and Soriano, 2003; Tallquist et al., 2000), sonic hedgehog (Shh) (Fan et al., 1995; Fan and Tessier-Lavigne, 1994; Johnson et al., 1994; Murtaugh et al., 1999; Zeng et al., 2002), and the BMP inhibitor Noggin (Nog) (Hirsinger et al., 1997; Marcelle et al., 1997; McMahon et al., 1998). The Flk1^{-}Pdgfrα^{+} rostral paraxial mesoderm from ESCs consistently show chondrogenic activity *in vitro* (Tanaka et al., 2009). However, it was not clear whether the paraxial mesoderm went through chondrogenesis via sclerotome specification, as occurs *in vivo*.

In addition, considering the necessity for culture scale-up for clinical application, there would be a significant cost benefit if the protein factors could be replaced with small-molecule signaling modifiers. Many chemical compounds have been developed that target relevant signaling mechanisms: e.g. the inhibitors of glycogen synthase kinase (Gsk)3, BIO (Sato et al., 2004) and CHIR99021 (Cohen and Goedert, 2004) for mimicking canonical Wnt signaling; SAG1 for mimicking hedgehog signaling (Chen et al., 2002), the dorsomorphin analog LDN193189 for inhibiting Alk1/2 and to a lesser degree Alk3 [type I BMP receptor (BMPR)] signaling (Yu et al., 2008), and SB431542 for inhibition of Alk4/5/7 (type I Nodal/activin/TGFβ receptor) signaling (Inman et al., 2002; Laping et al., 2002).

Here, we describe the establishment of a novel, small-molecule based differentiation method for the specification of chondrogenic rostral paraxial mesoderm from ESCs. We then demonstrate that the paraxial mesodermal progeny respond properly to a set of signals (hedgehog+Nog) known to be essential *in vivo* for generating sclerotome, and also specify sclerotome-like intermediates before forming chondrocytes *in vitro*. The same outcome was not recapitulated by TGFβ, which is used widely for the induction of chondrogenesis from various mesenchymal cell types. We have also demonstrated that the cartilage particles developed are mineralized and vascularized, leading to bone and marrow formation in a mouse model.

RESULTS

β-catenin activation without BMP signaling specifies chondrogenic rostral paraxial mesoderm from ESCs

During differentiation of the mouse brachyury (Bry)-GFP ESC in CDM, the presence of Wnt3a and Nog effectively induces rostral paraxial mesoderm but not lateral plate mesoderm in the Bry-GFP^{+}Flk1^{-}Pdgfrα^{+} cell fraction (Tanaka et al., 2009). Similarly, MIXL1-GFP^{+}KDR^{-}Pdgfrα^{+} paraxial mesoderm can be specified from Mixl1-GFP human ESCs in CDM in the presence of BIO and Nog (Umeda et al., 2012).

The canonical Wnt signaling mechanism involves suppression of Gsk3 activity and subsequent stabilization/nuclear translocation (hereafter described as 'activation') of β-catenin. Therefore, to confirm that canonical Wnt signaling is sufficient to induce paraxial mesoderm in the presence of Nog, we constructed the mouse ESC line, EBRβcatM, expressing the cDNA encoding a 4-hydroxy tamoxifen (OHT)-activatable β-catenin, i.e. Ctnnb1(S33Y)-Mer, in a tetracycline (Tet)-sensitive manner (supplementary material Fig. S1). The protein expression was monitored by the expression of yellow fluorescent protein (YFP). When the expression of Ctnnb (S33Y)-Mer protein was induced by lower concentrations of Tet from one day before differentiation and activation by OHT on day 2 of differentiation (Fig. 1A, supplementary material Fig. S2A), the expression of rostral paraxial mesoderm genes (e.g. *Meox1* and *Uncx*), but not lateral plate/extra-embryonic mesoderm genes (e.g. *Foxf1a* and *Hand2*) was induced by day 6 of differentiation (T/OHT, Fig. 1B, supplementary material Fig. S2B,C). The addition of Nog enhanced the level of paraxial mesoderm gene expression (T+N/OHT+N).

Under OHT+Nog, a significant level of YFP^{+}Flk1^{-}Pdgfrα^{+} progeny was generated (Fig. 1C). Similar to progeny generated under Wnt3a+Nog, the YFP^{+}Flk1^{-}Pdgfrα^{+} but not the YFP^{+}Flk1^{-}Pdgfrα^{-} cell fraction isolated by fluorescence-activated cell sorting (FACS) contained cells expressing paraxial mesodermal genes such as *Meox1* (Fig. 1C, supplementary material Fig. S2D left). Furthermore, cartilage nodule-forming activity was detected in the YFP^{+}Flk1^{-}Pdgfrα^{+} cell fraction generated under OHT+Nog during 2D micromass culture in the presence of PDGF+TGFβ (Fig. 1D, supplementary material Fig. S2E), as was seen in the Flk1^{-}Pdgfrα^{+} paraxial mesoderm generated under Wnt3a+Nog (Tanaka et al., 2009). By contrast, the YFP^{+}Flk1^{-}Pdgfrα^{+} progeny generated with OHT alone or with OHT+BMP4 resulted in significantly fewer cartilage nodules (Fig. 1D), similar to what was observed for the Pdgfrα^{+} lateral plate/extra-embryonic mesoderm fraction generated with either Wnt3a or BMP4 (Tanaka et al., 2009). Thus, the activated β-catenin is a substitute for Wnt3a signaling in the generation of chondrogenic paraxial mesoderm from ESCs.

Specification of chondrogenic paraxial mesoderm from ESCs by small molecules

Gsk3 occupies a crucial node in the mediation of various cellular processes (Hur and Zhou, 2010). However, the effects of Gsk3 suppression are considered to represent those of canonical, but not noncanonical, Wnt signaling that leads to β-catenin activation. Therefore, to complement the study involving overexpression of activated β-catenin (Fig. 1), the parental ESCs (EBRTcH3) were treated with various concentrations of three Gsk3 inhibitors: BIO, AcBIO or CHIR99021 (CHIR) (Fig. 2B). BIO stimulated *Meox1* expression by day 6 in a dose-dependent manner, but its inactive analog (MeBIO) did not (supplementary material Fig. S3E). Inclusion of Nog significantly enhanced the expression of *Meox1* in all cases (Fig. 2B left). Of the three inhibitors, CHIR had the strongest effect on the induction of *Meox1* transcript (peaking at 5 μM), but at >5 μM induced significant levels of *Meox1* even in the absence of Nog (CN, C). Thus, the overexpressed, activated β-catenin could be effectively replaced with either Gsk3 inhibitor, BIO or CHIR.

We next attempted to replace the pan-BMP inhibitor Nog, which prevents BMPs from binding to BMPRs, with the Alk1/2/(3)-inhibitor, LDN193189 (LDN). At about 0.6 μM, LDN augmented the CHIR-induced expression of *Meox1* during ESC differentiation (Fig. 2B right). The enhancement of *Meox1* expression with Nog or LDN was more pronounced with 5 μM CHIR than with BIO or 2.5 μM CHIR. Furthermore, similar to Wnt3a+Nog (Tanaka et al., 2009), CHIR+LDN also induced the formation of Flk1^{-}Pdgfrα^{+} progeny from EBRTcH3 and Bry-GFP ESCs. The Flk1^{-}Pdgfrα^{+} cells were Bry-GFP^{+} (Tanaka et al., 2009), suggesting mesendodermal origin, and the majority of them were E-cadherin^{-} (Fig. 2C), i.e. mesoderm. Consistently, the E-cadherin^{-}Bry^{+}Flk1^{-}Pdgfrα^{+} progeny, but not the E-cadherin^{-}Bry^{+}Flk1^{-}Pdgfrα^{-} progeny isolated by FACS were enriched in the rostral paraxial mesoderm transcripts *Meox1*, *Tcf15* and *Uncx* (see Fig. 3C, supplementary material Fig. S5C), and were also found to be chondrogenic in the subsequent micromass culture (Fig. 2C). Thus, LDN could effectively replace Nog, although

Development (2014) 141, 3848-3858 doi:10.1242/dev.105981

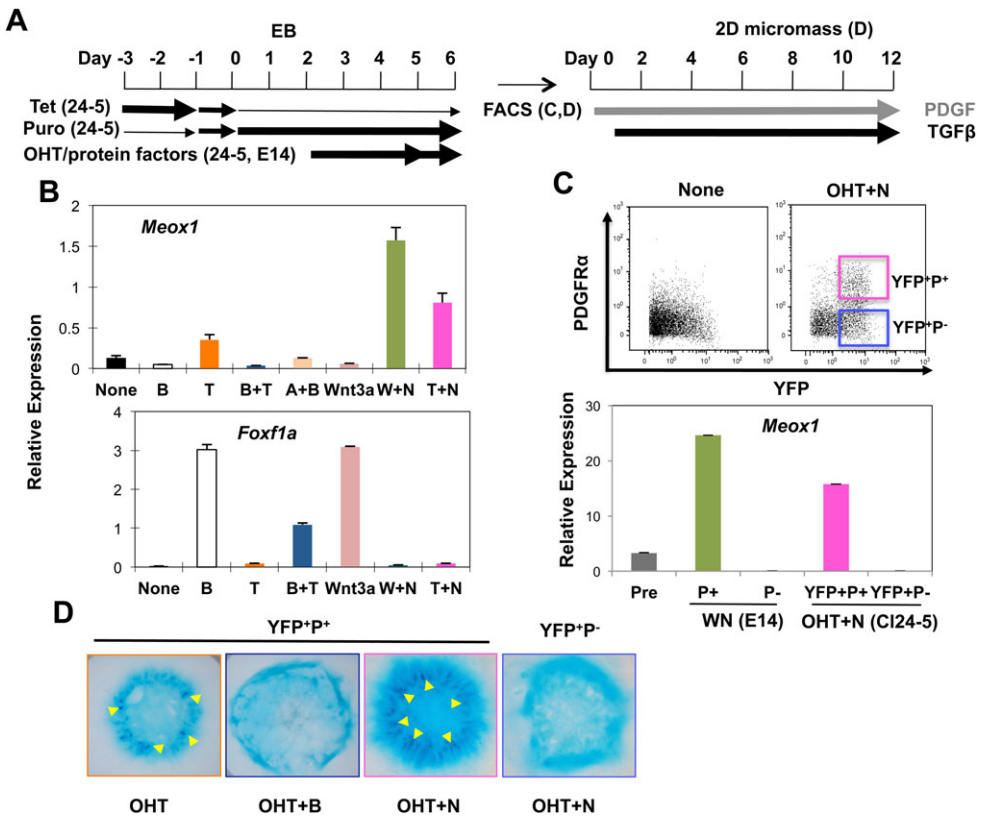

Fig. 1. Activated β-catenin and Nog generate chondrogenic paraxial mesoderm from ESCs. (A) Experimental scheme. EBRβcatM (Cl24-5; indicated by '24-5') and E14 ESCs were differentiated for 6 and 5 days, respectively. The change in the thickness of arrows indicates reduction or increase in the concentrations of indicated reagents. (B) EBRβcatM (Cl24-5) cells were differentiated with the indicated factors. RT-PCR analysis was conducted using *Meox1* and *Foxf1a* primers. None: no factor, A: activin 25 ng/ml, B: BMP4, T: OHT, W: Wnt3a, N: 500 ng/ml Nog. (C) EBRβcatM (Cl24-5) cells and E14 ESCs were differentiated with the indicated factors. $YFP^+Flk1^-Pdgfr\alpha^+$ (YFP^+P^+) and $YFP^+Flk1^-Pdgfr\alpha^-$ (YFP^+P^-) progeny were isolated from the former, and $Flk1^-Pdgfr\alpha^+$ (P^+) and $Flk1^-Pdgfr\alpha^-$ (P^-) progeny were form the latter, respectively, by FACS. RT-PCR analysis was performed with the *Meox1* primers. Pre: total OHT+N treated EB cells, OHT+N: OHT and 500 ng/ml Nog, WN: Wnt3a and 500 ng/ml Nog. (D) Chondrogenic activity of the activated β-catenin-induced progeny. EBRβcatM (Cl24-5) ESCs were differentiated with the indicated factors. YFP^+P^+ and YFP^+P^- progeny were isolated by FACS and subjected to micromass culture in the presence of PDGF and TGFβ as described (Nakayama et al., 2003; Tanaka et al., 2009). Cultures were fixed on day 12, and stained with acid Alcian Blue. OHT+B: OHT and 1 ng/ml BMP4. Typical dark blue spots (signs of chondrogenesis) in OHT and in OHT+N are highlighted with yellow arrowheads.

LDN preferentially inhibited Alk1/2 instead of the classical type I BMPR Alk3/6 (Yu et al., 2008).

Nodal signaling is involved in gastrulation and germ layer specification in a dose-dependent manner (Schier, 2009). By day 5 of ESC differentiation, Wnt3a, and to a lesser degree BIO, induced expression of the *Nodal* gene via a pathway independent of BMP signaling, as shown by the lack of effect of Nog (supplementary material Fig. S3B,C right). This finding revealed the potential to optimize differentiation by manipulating Nodal signaling using activin A (activin) and the Nodal/activin/TGFβ receptor inhibitor SB431542 (SB). Attempts to optimize the differentiation method using activin and SB resulted in a parabolic response (Fig. 2D) similar to that seen with EBRβcatM cells (supplementary material Fig. S2D right). The optimal concentrations fell within a small range from 0-5 ng/ml activin to 0-1 μM SB, depending on the type of Wnt activator used. Furthermore, inefficient specification of Meox1-expressing paraxial mesoderm in the presence of activin at higher concentrations (5-20 ng/ml) correlated with the reduction in the $Flk1^-Pdgfr\alpha^+$ cell population in EBs formed, and with the weak to nonexistent chondrogenic activity in the $Bry^+Flk1^-Pdgfr\alpha^+$ progeny (Fig. 2E). Interestingly, in specification of paraxial mesoderm the use of Gsk3 inhibitors gave consistently higher levels of *Meox1* transcript than the use of Wnt3a in the presence of Nog (Fig. 2D). However, under the optimal small-molecule condition [5 μM CHIR +0.6 μM LDN (CHIR+LDN)], *Meox1* was induced at levels statistically equivalent to those achieved under the protein-based, Wnt3a+Nog condition (supplementary material Fig. S5B).

These results indicate that small-molecule inhibitors of Gsk3 and BMPR successfully replace Wnt3a and Nog for efficient specification of chondrogenic, rostral paraxial mesoderm from ESCs. Manipulation of Nodal/activin/TGFβ signaling is not always necessary, but must be a special consideration when differentiation efficacy is of a critical matter (supplementary material Fig. S4).

Specification of sclerotome from ESCs via a rostral paraxial mesoderm intermediate

Early expression of Pax1 among the mesodermal progeny is largely restricted to the ventral part of sclerotome (Deutsch et al., 1988; Koseki et al., 1993), which is induced by the diffusible factors Shh and Nog, produced from the floor plate and the notochord. The $Flk1^-Pdgfr\alpha^+$ rostral paraxial mesoderm induced from ESCs in KSR-based serum-free medium expressed *Pax1* mRNA (Tanaka et al., 2009), but those induced in CDM under either Wnt3a+Nog (data not shown) or CHIR+LDN (CL, Fig. 3B,C, supplementary material Fig. S5C) seemed to lack *Pax1* mRNA despite *Meox1*, *Tcf15* and *Uncx* transcripts being highly enriched. We therefore examined the effect of hedgehog on the expression of Pax1 during differentiation of

Development (2014) 141, 3848-3858 doi:10.1242/dev.105981

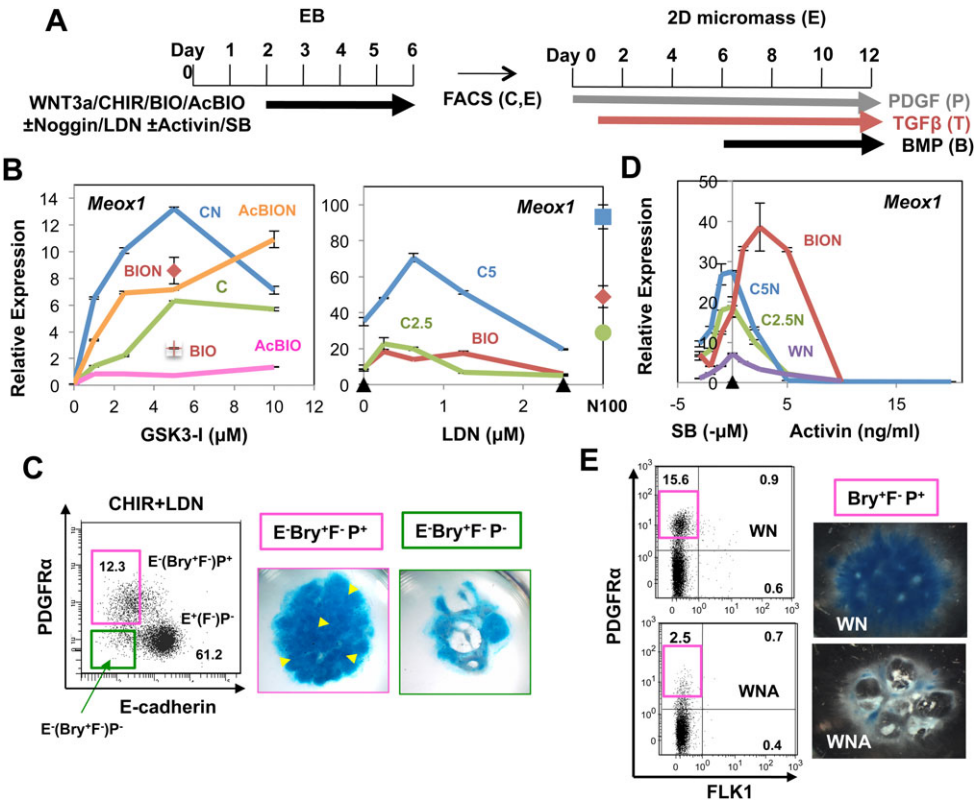

Fig. 2. Effects of small-molecule signaling-modifiers on rostral paraxial mesoderm specification. (A) Experimental scheme. (B) Dose-dependent effects of Gsk3 inhibitors and BMP inhibitors on *Meox1* induction. (Left panel) EBRTcH3 cells were differentiated in the presence of various concentrations of CHIR (C, blue and green) and AcBIO (orange, pink) with (blue, orange) or without (green, pink) Nog (N). RT-PCR was performed on total EB cells. Cross: 5 μM BIO, Rhombus: BION. (Right panel) Dose-dependent effect of LDN193189 on *Meox1* expression compared with the effect of Nog. Various concentrations of LDN or 100 ng/ml Nog (N100) were added in the presence of no factor (black triangle), BIO (brown), 2.5 μM CHIR (C2.5, green) and 5 μM CHIR (C5, blue). RT-PCR was performed on day 6 EBs. (C) Chondrogenic activity of the paraxial mesodermal progeny. Bry-GFP cells were differentiated with 5 μM CHIR and 0.6 μM LDN (CHIR+LDN), and E-cadherin$^-$Bry$^+$Flk1$^-$Pdgfrα$^+$ (E$^-$Bry$^+$F$^-$P$^+$) and E-cadherin$^-$Bry$^+$Flk1$^-$Pdgfrα$^-$ (E$^-$Bry$^+$F$^-$P$^-$) progeny were FACS purified (left panel), which were then subjected to micromass culture under PT→PTB (PDGF+TGFβ→[from day 6] PDGF+TGFβ+BMP) conditions (right panel). Typical dark blue spots are highlighted with yellow arrowheads. (D) Dose-dependent effects of Nodal/activin/TGFβ signaling on the *Meox1* expression. EBRTcH3 cells were differentiated in the presence of no factor (black triangle), Wnt3a +300 ng/ml Nog (WN), BIO+Nog (BION), 2.5 μM CHIR+Nog (C2.5N), and 5 μM CHIR+Nog (C5N), together with various concentrations of activin and SB. As SB suppresses endogenous Nodal/activin/TGFβ signaling, the dose-dependent effect is plotted as '−μM' in the negative range. (E) Chondrogenic activity of the (paraxial) mesodermal progeny generated in the presence of a high concentration of activin. Bry-GFP cells were differentiated in the presence of Wnt3a +500 ng/ml Nog (WN) with or without 20 ng/ml activin (A), and Bry$^+$Flk1$^-$Pdgfrα$^+$ (Bry$^+$F$^-$P$^+$) progeny (left panel, pink) were sorted as described before (Tanaka et al., 2009). The isolated cells were individually subjected to micromass culture under PDGF+TGFβ conditions (Nakayama et al., 2003; Tanaka et al., 2009).

ESCs in CDM. The small-molecule SMO (hedgehog receptor subunit)-agonist SAG1 (SAG) was used to activate hedgehog signaling. The addition of SAG to the (CHIR+LDN)-based differentiation culture on day 4 significantly upregulated Pax1 expression by day 6 (CLS4, Fig. 3B), but had only marginal effects on Meox1 expression and no effect on the progenitor profile distinguished by Flk1 and Pdgfrα expression (data not shown). Consistently, the FACS-purified E-cadherin$^-$Flk1$^-$Pdgfrα$^+$ cell fraction thus generated was enriched in *Pax1* mRNA (i.e. sclerotome) and *Meox1*, *Tcf15* and *Uncx* transcripts (i.e. rostral paraxial mesoderm) (Fig. 3C, supplementary material Fig. S5C). The induction of *Pax1* occurred more slowly or to a lesser extent when SAG was added on day 2 instead of day 4 (CLS2, Fig. 3B).

When both Bry$^+$Flk1$^-$Pdgfrα$^+$ and Bry$^+$Flk1$^-$Pdgfrα$^-$ progeny were isolated by FACS from EBs developed from Bry-GFP ESCs under CHIR+LDN, and subjected to micromass culture in the presence of Shh+Nog with PDGF, only the Bry$^+$Flk1$^-$Pdgfrα$^+$ cells were capable of inducing the sclerotomal genes *Bapx1* (Tribioli et al., 1997) and *Pax1* as well as the more committed chondroprogenitor gene *Sox9* within 6 days (Fig. 3D). Therefore, the Pax1-expressing sclerotomal cells were probably generated from Pax1-negative Flk1$^-$Pdgfrα$^+$ rostral paraxial mesoderm.

Transient treatment with small-molecule SMO agonist and BMPR inhibitor allows exogenous TGFβ-independent chondrogenesis from the isolated rostral paraxial mesoderm

To demonstrate that the Pax1-positive Flk1$^-$Pdgfrα$^+$ sclerotomal cells are qualitatively more chondrogenic than the immediate precursor cells: i.e. Pax1-negative Flk1$^-$Pdgfrα$^+$ rostral paraxial mesoderm, we first isolated them individually from EBs generated in CDM under CHIR+LDN+SAG (day 4) and CHIR+LDN conditions, respectively, and performed micromass culture in the presence of PDGF, TGFβ and BMP4. However, no significant difference in the efficiency of chondrogenesis was observed (data not shown). The exposure to SAG for 2 days (from day 4 to day 6) during ESC differentiation might be too short to promote commitment of sufficient rostral paraxial mesodermal cells to sclerotome.

Therefore, we isolated the Pax1-negative Flk1$^-$Pdgfrα$^+$ rostral paraxial mesoderm, and addressed whether treatment with Shh

Development (2014) 141, 3848-3858 doi:10.1242/dev.105981

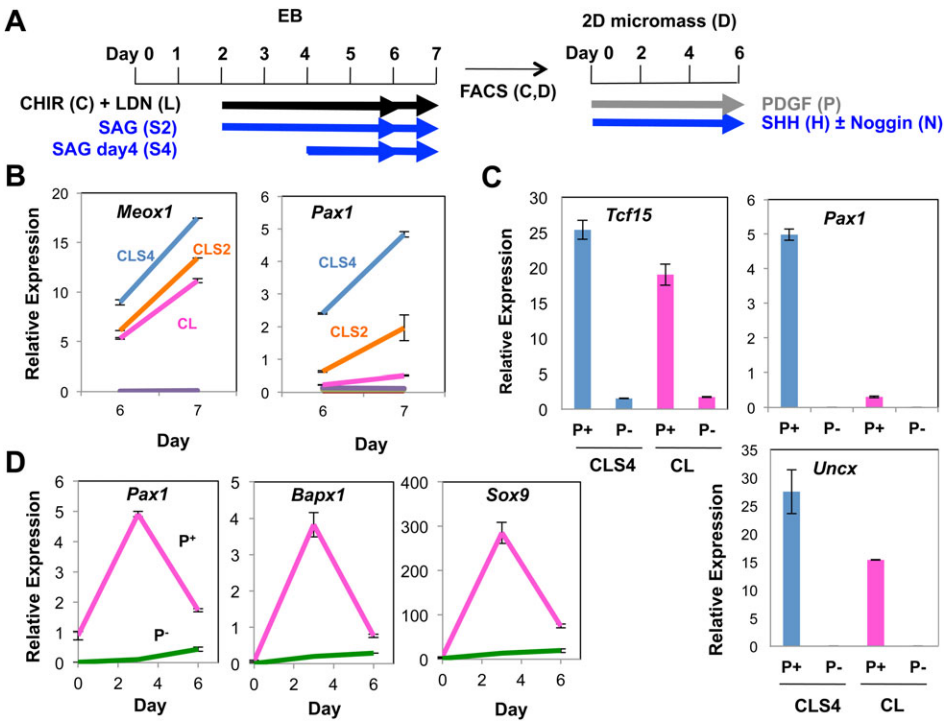

Fig. 3. Hedgehog and small-molecule SMO agonist for sclerotome specification from ESCs. (A) The experimental scheme. (B) EBRTcH3 cells were differentiated under no factor (purple), CHIR (C, green), CHIR +LDN (CL, pink), CHIR+LDN+SAG (day 2) (CLS2, orange) and CHIR+LDN+SAG (day 4) (CLS4, blue). RNA was extracted on days 6 and 7, and subjected to RT-PCR using *Meox1* and *Pax1* primers. (C) EBRTcH3 cells were differentiated for 6 days under CL and CLS4, and the E-cadherin^{-}Flk1^{-}Pdgfrα^{+} (P^{+}) and Flk1^{-}Pdgfrα^{-} (P^{-}) progeny were isolated by FACS on day 6 and subjected to RT-PCR using *Tcf15*, *Pax1* and *Uncx* primers. (D) Bry-GFP cells were differentiated under CL, and the Bry^{+}Flk1^{-}Pdgfrα^{+} (P^{+}, pink) and Bry^{+}Flk1^{-}Pdgfrα^{-} (P^{-}, green) progeny were sorted and subjected to micromass culture in the presence of PDGF+hedgehog+Nog. Cultures were harvested on days 3 and 6 for RT-PCR analysis.

+Nog or with their small-molecule analogues SAG+LDN for a longer time would affect the efficiency of chondrogenesis. The 12-day micromass cultures were performed under the following four different conditions, all of which included PDGF (P) as a growth/viability-supporting factor: (1) PHN→PB: Shh+Nog for 6 days (as in Fig. 3D) then BMP4 for 6 days, (2) PSL→PB: SAG+LDN for 6 days then BMP4 for 6 days, (3) PTHN→PTB: condition 1 plus TGFβ, and (4) PTSL→PTB: condition 2 plus TGFβ, with appropriate controls (Fig. 4B). The chondrogenesis cultures with TGFβ (PT→PT), but not those without TGFβ (P→P), generated micromass stained with Alcian Blue. Later (i.e. day 6) addition of BMP4 to the PT culture (PT→PTB) enhanced chondrogenesis as

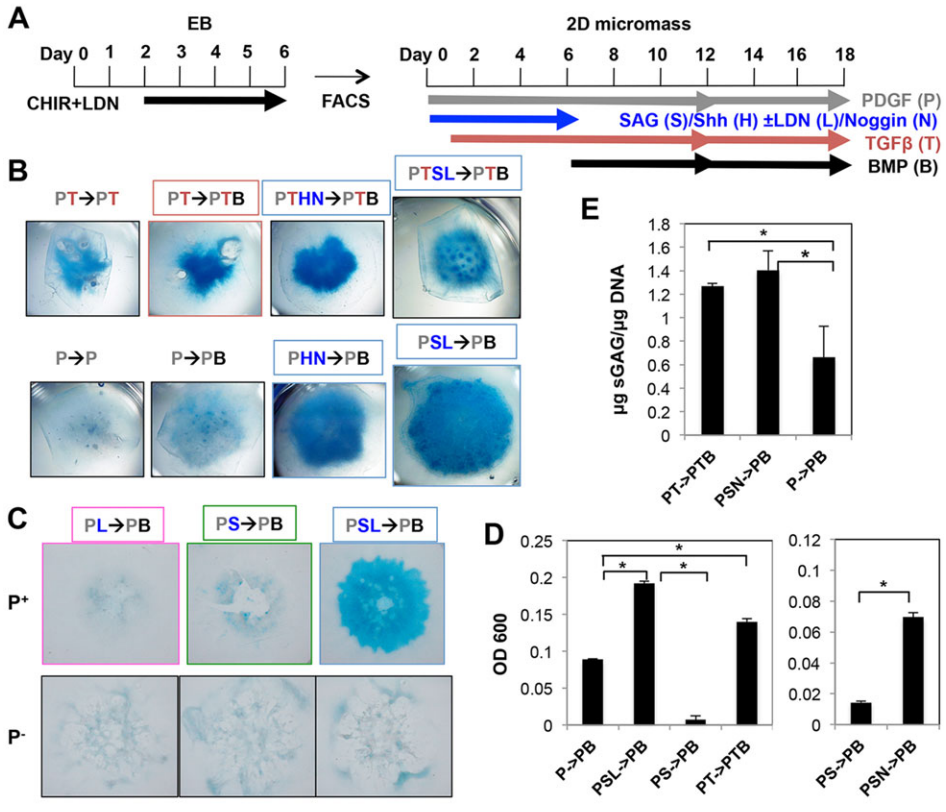

Fig. 4. Small-molecule-facilitated chondrogenesis from the isolated rostral paraxial mesoderm. (A) Experimental scheme. EBRTcH3 ESCs were differentiated under CHIR+LDN. (B) Effects of protein factors versus small molecules (Shh versus SAG, and Nog versus LDN) on chondrogenesis. Micromass cultures were performed with the sorted E-cadherin^{-}Flk1^{-}Pdgfrα^{+} progeny under the conditions indicated. Conditions; P: PDGF, T: TGFβ, B: BMP4, H: Shh, N: Nog, S: SAG, L: LDN, →: factor change on day 6. (C) Requirement for both SAG and LDN. The E-cadherin^{-}Flk1^{-}Pdgfrα^{+} (P^{+}) and Flk1^{-}Pdgfrα^{-} (P^{-}) progeny were isolated and subjected to micromass culture under PL, PS and PSL conditions, and then PB from day 6. The cultures (B,C) were then fixed on day 12, and stained with acid Alcian Blue. (D) Quantification of bound Alcian Blue. The E-cadherin^{-}Flk1^{-}Pdgfrα^{+} progeny were subjected to micromass culture under the indicated conditions for 12 days. After fixation and Alcian Blue staining, the bound Alcian Blue was extracted from each micromass, and quantified by OD600. *P<0.05. (E) Quantification of sGAG. The E-cadherin^{-}Flk1^{-}Pdgfrα^{+} progeny were subjected to micromass culture for 18 days under the indicated conditions. The total DNA and sGAG were quantified (supplementary material Fig. S6G), and normalized values (μg sGAG/μg DNA) are displayed. *P<0.05.

Development (2014) 141, 3848-3858 doi:10.1242/dev.105981

shown by darker blue staining. No such enhancement was observed without TGFβ (P→PB). Interestingly, even in the absence of TGFβ, conditions 1 (PHN→PB) and 2 (PSL→PB) gave rise to a large micromass that stained strongly with Alcian Blue. The micromass accumulated similar amounts of sulfated glycosaminoglycan (sGAG), as judged by the guanidine hydrochloride-extractable Alcian Blue per mass, as that developed under PT→PTB (Fig. 4D). Furthermore, the micromasses developed under PT→PTB and PSN→PB (SAG+Nog followed by BMP4, similar to condition 2) conditions for 18 days contained a similar proportion of active chondrocytes, as indicated by sGAG normalized to DNA, but significantly more than those developed under P→PB conditions (Fig. 4E). The yield of DNA from a micromass reflects cell number, which did not differ significantly at this stage (supplementary material Fig. S6G).

The PSL→PB as well as PSN→PB conditions favor exogenous TGFβ-independent chondrogenesis from the Flk1^{-}Pdgfrα^{+} rostral paraxial mesoderm, but not from the Flk1^{-}Pdgfrα^{-} progeny (Fig. 4C, supplementary material Fig. S6D). The later treatment with BMP4 proved important. Without it, the efficiency of overall chondrogenesis was reduced significantly (PSL→P, supplementary material Fig. S6E,F). Addition of both SAG and LDN/Nog during the first 6 days of micromass culture was also essential, as treatment with either SAG (PS→PB) or LDN (PL→PB) resulted in zero or only very weak chondrogenesis (Fig. 4C,D, supplementary material Fig. S6C,D,F), with a small change in the growth of micromass (data not shown).

(SAG+Nog/LDN)-induced, but not TGFβ-induced, chondrogenesis from rostral paraxial mesoderm proceeded via sclerotome specification

Real-time RT-PCR analyses demonstrated that SAG+LDN (PSL) stimulation during the first 6 days of micromass culture was crucial for inducing *Pax1* and *Bapx1* expression from the isolated E-cadherin^{-}Flk1^{-}Pdgfrα^{+} rostral paraxial mesoderm (Fig. 5B), as was the Shh+Nog stimulation (Fig. 3D). Both transcripts were highly induced at around day 3 by either treatment, but not by treatment with TGFβ (PT, Fig. 5B), LDN (PL) or SAG (PS) alone. The PSL treatment should continue for longer than 3 days before the change to PDGF+BMP4 (PB), and consistent with the notion that BMP signaling counteracts Shh+Nog and inhibits sclerotome induction (Dockter, 2000), an early (day 3) transition led to a somewhat weaker degree of chondrogenesis (supplementary material Fig. S6B). By contrast, expression of *Sox9* was strongly induced under PT and somewhat weakly induced under PSL within the first 6 days, but was not induced under PS conditions. In support of differentiation toward chondrocytes, the somite transcript *Uncx* also disappeared.

These differences in the sclerotomal gene expression during early micromass culture might simply reflect different kinetics of induced chondrogenesis, such that the sclerotomal genes *Pax1* and *Bapx1* might be expressed at a later time under PT conditions. Therefore, the entire chondrogenesis process was monitored. As LDN shows BMPR subtype specificity (Yu et al., 2008), the SAG+Nog (PSN) condition was included as a control. As shown in Fig. 5C and supplementary

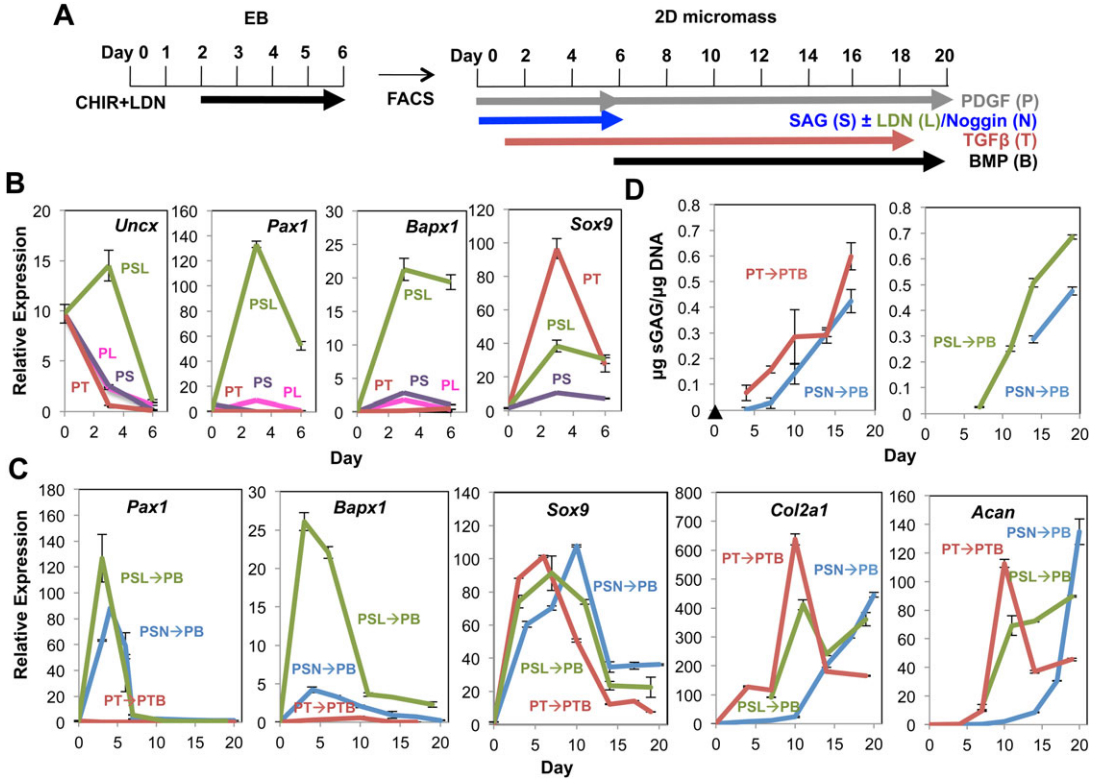

Fig. 5. Different mechanism of chondrogenesis initiated with SAG+LDN or TGFβ from the isolated paraxial mesoderm generated. (A) Experimental scheme. EBRTcH3 ESCs were differentiated under CHIR+LDN, and the E-cadherin^{-}Pdgfrα^{+} progeny were isolated. (B) Sclerotome specification by small molecules. The micromass cultures were initiated under P (black), PS (purple), PL (pink), PSL (green) and PT (brown) conditions. Cultures were harvested on days 3 and 6 for RT-PCR with the indicated primers. Conditions; P: PDGF, T: TGFβ, B: BMP4, H: Shh, N: Nog, S: SAG, L: LDN. (C) Differential chondrogenic programs. The micromass cultures performed for 19-20 days under PSL→PB (green), PSN→PB (blue) and PT→PTB (brown) conditions were periodically harvested for RT-PCR with the indicated primers. (D) Quantification of sGAG. The micromass cultures performed under the same conditions as in C were subjected to total DNA and sGAG quantification (supplementary material Fig. S8B), and normalized values (μg sGAG/μg DNA) are displayed. Black triangle: freshly sorted cells.

Development (2014) 141, 3848-3858 doi:10.1242/dev.105981

material Fig. S7B, under PSL/PSN→PB conditions, *Pax1* and *Bapx1* expression was induced and peaked within the first 6 days (i.e. before BMP4 stimulation), consistent with the previous results (Fig. 3D and Fig. 5B). *Pax1* and *Bapx1* expression then significantly decreased or disappeared by day 7 and day 11, respectively, and did not reappear by day 19. Both the type II collagen (*Col2a1*) and aggrecan (*Acan*) transcripts, the signs of chondrocyte formation, were detectable from days 11-14 under PSN→PB and from approximately day 6 under PSL→PB. By contrast, under PT→PTB conditions, *Pax1* and *Bapx1* expression was scarcely detectable until days 19-20, but *Col2a1* and *Acan* transcripts were detectable by day 6, and the levels peaked at around day 11. *Sox9* expression was detected under both PSL/PSN→PB and PT→PTB conditions, as with the previous observations (Fig. 3D and Fig. 5B). However, whereas the *Sox9* level peaked by day 6 under PT→PTB, *Sox9* was expressed over a longer period under PSL/PSN→PB, and especially under PSN→PB for which the peak was delayed to days 7-11 (Fig. 5C, supplementary material Fig. S7B). Concomitantly, *Col2a1* and *Acan* transcripts were induced significantly earlier under PT→PTB than under PSN→PB, but kinetic differences between PT→PTB and PSL→PB conditions were not clear (Fig. 5C, supplementary material Fig. S7C). Thus, the transition from early expression of *Pax1* and *Bapx1* to later expression of *Sox9*, *Col2a1* and *Acan* was apparent under the PSL/PSN→PB conditions, while induction of *Sox9*, *Col2a1* and *Acan* without expression of *Pax1* and *Bapx1* was observed under PT→PTB condition.

Furthermore, quantitation of sGAG (normalized to DNA) indicated that the micromass developed under both PSL/PSN→PB and PT→PTB conditions accumulated proteoglycan-producing active chondrocytes (Fig. 5D). Consistently under PSN→PB conditions (blue) such active chondrocytes accumulated more slowly than those under PT→PTB (brown) and PSL→PB (green) conditions.

Thus, the ESC-derived rostral paraxial mesoderm can give rise to chondrocytes through two different developmental programs: one initiated by SAG and LDN/Nog (PSL/PSN), which involves Pax1 and Bapx1 induction, i.e. sclerotome specification, and the second by TGFβ (PT), which does not involve sclerotome specification. Interestingly, the PSL→PB condition tended to induce Pax1 and Bapx1 more efficiently and show faster chondrogenesis than the PSN→PB condition, implying that inhibition of Alk1/2-dependent BMP signaling may be the key for sclerotome specification *in vitro*.

Capacity of the macroscopic cartilage particles developed from rostral paraxial mesoderm via different chondrogenesis mechanisms to mature *in vitro* and *in vivo*

Different chondrogenesis programs might lead to different cartilage types. As BMP4 is a robust chondrogenic inducer for many mesenchymal cell types but is also known to facilitate terminal maturation of the developed chondrocytes, we addressed whether chondrocytes developed from the rostral paraxial mesoderm during micromass culture under the conditions in which Pax1 and Bapx1were induced (PSL/PSN→PB) and not induced (PT→PTB) would differentially express the *Col10a1* and *Alpl* transcripts, a sign of hypertrophic differentiation (Fig. 6B, supplementary material Fig. S7B,C). Chondrocytes generated under all conditions expressed *Col10a1* and *Alpl* slightly later than *Col2a1* and *Acan*

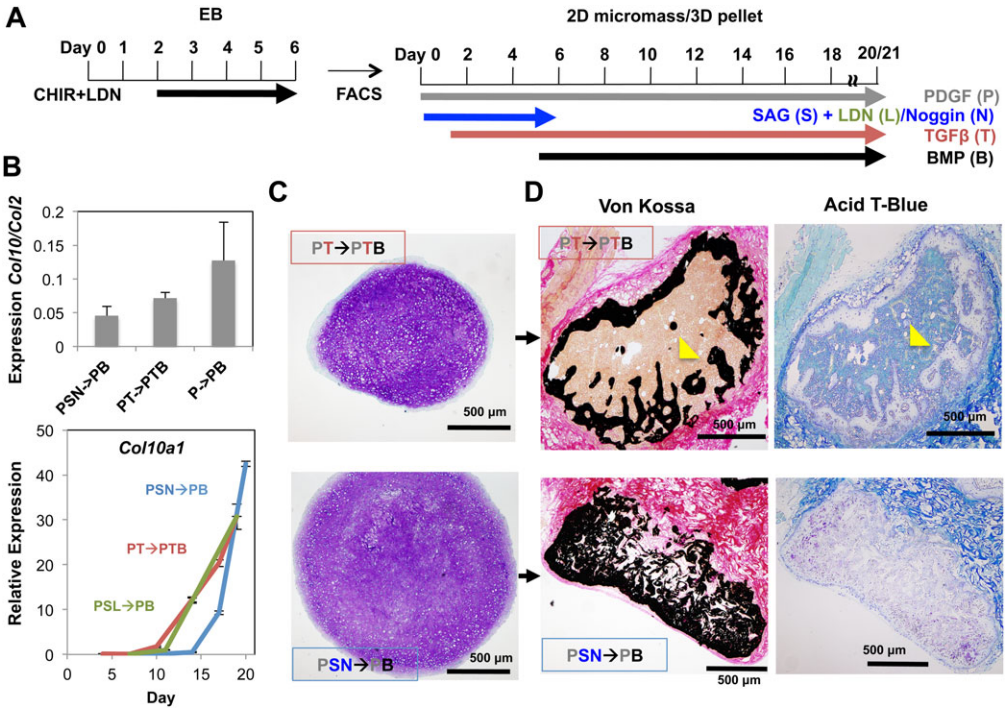

Fig. 6. Stability of the cartilage formed with the ESC-derived rostral paraxial mesoderm. (A) Experimental scheme. EBRTcH3 ESCs were differentiated under CHIR+LDN, and the E-cadherin^{-}Pdgfrα^{+} progeny were isolated. (B) The micromass cultures were performed for 19-20 days under PSL→PB (green), PSN→PB (blue), PT→PTB (brown) and P→PB conditions and were periodically harvested for RT-PCR with primers for *Col10a1* and *Col2a1*. The ratio of *Col10a1* (*Col10*) to *Col2a1* (*Col2*) was calculated based on the day 20 results (supplementary material Fig. S8C). Conditions; P: PDGF, T: TGFβ, B: BMP4, N: Nog, S: SAG, L: LDN, →: factor change on day 6. (C) Cartilage particles generated under PT→PTB and PSN→PB in 21 days. Toluidine Blue (T-Blue) staining. (D) The cartilage particles from (C) were transplanted subdermally for 12 weeks after which the resulting particles were fixed, plastic embedded, sectioned. The sections were subjected to von Kossa-van Gieson staining (left panels) and acid T-Blue staining (right panels). The von Kossa stains bony, mineralized area black. T-blue stains the cartilaginous area purple and other areas blue. The upper panels show mineralized bone-like tissue with hematopoietic marrow. The yellow triangle indicates the area with blood cells.

Development (2014) 141, 3848-3858 doi:10.1242/dev.105981

(Fig. 5C). Similarly, the kinetics of expression under PSL→PB and PT→PTB were faster than under PSN→PB. However, the ratio of the normalized levels of *Col2a1* and *Col10a1* transcripts accumulated under PT→PTB and PSN→PB conditions did not differ significantly (Fig. 6B upper), suggesting that the rate of maturation of the developed chondrocytes is indistinguishable under both conditions.

In addition, using the 3D pellet culture method, we made cartilage particles under PSN→PB and PT→PTB conditions (Fig. 6C,D). The resulting particles were indistinguishable in size and degree of chondrogenesis, as judged by histological examination. Multiple sections of individual particles demonstrated that all consisted of cartilaginous area that stained uniformly with Toluidine Blue. When such particles were transplanted subcutaneously into immunocompromised mice, both developed in 12 weeks into vascularized and mineralized tissues that contained bone-like structure with hematopoietic marrow. Nog, not LDN, is one of the authentic sclerotome inducers *in vivo*, and PSN→PB, not PSL→PB, resulted in a significant difference in the kinetics of chondrogenesis compared with PT→PTB (Fig. 5C,D and Fig. 6B). Interestingly, however, the cartilage particles made under PSL→PB conditions yielded essentially the same mineralized cartilage (supplementary material Fig. S8D,E). These observations suggest that the chondrocytes produced from the rostral paraxial mesoderm under both PSL/PSN→PB and PT→PTB conditions resemble growth plate chondrocytes in being able to go through endochondral ossification.

DISCUSSION

We have demonstrated that small-molecule signaling-modifiers that inhibit Gsk3 and type I BMPR and promote hedgehog signaling effectively specify rostral paraxial mesoderm and then sclerotomal progeny from mouse ESCs as the corresponding protein factors. Therefore, it is now feasible to scale up the culture to obtain a large number of these progeny. We have also demonstrated that chondrocytes can be generated from isolated rostral paraxial mesoderm through two developmental mechanisms (Fig. 7) – the authentic (Shh+Nog)-initiated somitic chondrogenesis mechanism through sclerotome specification, and the TGFβ-induced chondrogenesis mechanism with no sign of sclerotome specification.

In sclerotome, Pax1 and Pax9 interact with Meox1 to induce Bapx1 (Nkx3.2) expression (Rodrigo et al., 2004, 2003). This leads to activation of the Bapx1-Sox9 positive-feedback mechanism that allows sclerotome to respond to BMP signaling and differentiate into chondrocytes (Kempf et al., 2007; Tribioli and Lufkin, 1999; Yamashita et al., 2009; Zeng et al., 2002). Thus, Bapx1 is crucial for chondrocyte formation for developing vertebral bodies and intervertebral discs (Akazawa et al., 2000; Herbrand et al., 2002; Lettice et al., 1999). The protein (i.e. Shh+Nog)-induced or small-molecule (i.e. SAG+LDN)-induced Pax1 and Bapx1 expression followed by Sox9 expression and BMP4-enhancement of chondrogenesis, therefore, suggests that mouse ESC-derived rostral paraxial mesoderm possesses the capacity of going through the somitic chondrogenesis program as embryonic somitic mesoderm (Dockter, 2000). By contrast, the TGFβ-induction of Sox9 and BMP4-enhancement of chondrogenesis without Pax1 and Bapx1 expression suggests that paraxial mesodermal chondrogenesis can also proceed directly without the Bapx1-Sox9 positive-feedback mechanism.

The conditions in which TGFβ and BMP are involved have been widely used for inducing chondrogenesis *in vitro* from a variety of mesenchymal cells. In chick embryos, induction of Sox9 expression and chondrogenesis by Shh or by forced Bapx1 expression is observed specifically in paraxial mesoderm (Kempf et al., 2007; Zeng et al., 2002). The same treatments of lateral plate mesoderm fail to induce chondrogenesis. However, forced Sox9 expression allows chondrogenesis from both mesodermal types. These findings suggest that exogenous TGFβ may directly induce Sox9 in many mesenchymal cell types, leading to rapid chondrogenesis *in vitro*.

The two different mechanisms of chondrogenesis may be mediated by two types of chondrogenic cell present in the rostral paraxial mesoderm fraction, or by one cell type (i.e. sclerotome) with dual capacity. Evidence suggests that the latter is more likely. More than 97% of the cells in the E-cadherin^{-}Flk1^{-}Pdgfrα^{+} rostral paraxial mesoderm fraction were Bry-GFP^{+}, in which no sign of lateral plate mesoderm and neural crest specification was detected, and both conditions commonly give rise to chondrocytes with the tendency to ossify (Fig. 6).

The question arises as to the importance of the slower and more complex 'somitic chondrogenesis' program over the faster and simpler 'TGFβ-induced chondrogenesis program'. Bone and cartilage

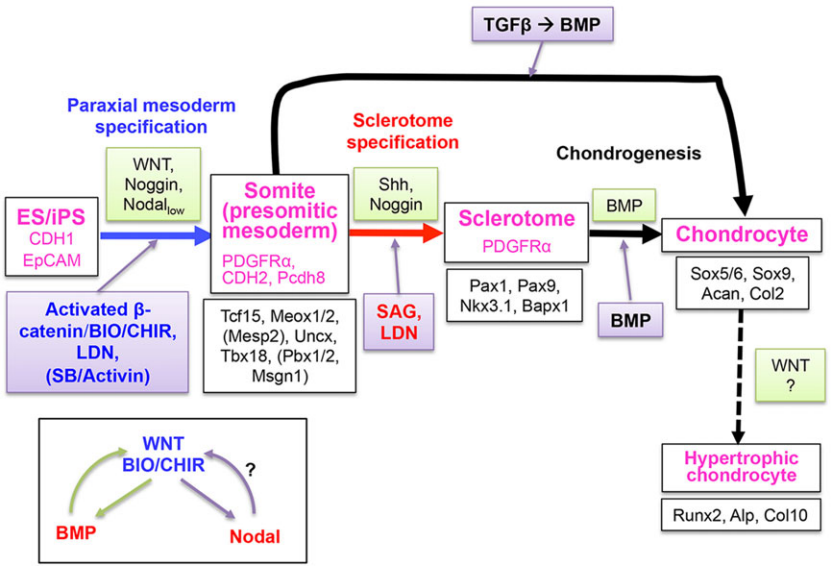

Fig. 7. Schematic diagram for pharmacological regulation of sclerotome specification and induction of somitic chondrogenesis from ESCs. Mesoderm specification, sclerotomal cell specification and chondrogenesis are indicated in blue, red and black arrows, respectively. The growth factors in green boxes are those that have proved essential for the indicated step during embryogenesis. The pharmacological agents and growth factors in purple boxes are those we have found to be sufficient for the indicated step *in vitro*. Based on the results presented in supplementary material Fig. S3 and Tanaka et al. (2009), positive-feedback relations in the production of Wnt, BMP and Nodal from EB cells during paraxial mesoderm specification are illustrated in the lower-left box.

Development (2014) 141, 3848-3858 doi:10.1242/dev.105981

formation during embryogenesis is under a tight spatiotemporal control to ensure development of the correct skeletal structure at the correct place. One possible advantage is to make the somitic chondrogenesis process more controllable by extracellular environment. Furthermore, as Bapx1 suppresses Runx2, which is associated with hypertrophic differentiation and subsequent mineralization of chondrocytes (Provot et al., 2006), the Bapx1-Sox9 positive-feedback loop might serve as a mechanism for maintenance of chondrocytes in the nonmineralizing state, as observed in the stable intervertebral disc cartilage. Unfortunately, the results of ectopic transplantation did not support this hypothesis (Fig. 6C,D, supplementary material Fig. S8D,E).

However, the ESC-derived paraxial mesoderm is similar to *in vivo* paraxial mesoderm, in that both sense the same set of developmental signals (hedgehog/SAG and Nog/LDN) and respond to them in the same way (sclerotomal specification then chondrocyte formation) as *in vivo*. Such signal-controllable differentiation capacity, together with the fact that many of the skeletogenic signaling mechanisms to which the ESC-derived paraxial mesoderm is expected to respond have already been elucidated, will place the cell system described in an advantageous position over other (adult cell) systems when it comes to finding a suitable condition for the formation and/or regeneration of stable cartilage. As for future therapeutic application, we have already reported the generation of chondrogenic paraxial mesodermal cells from human PSCs using a Gsk3 inhibitor (Umeda et al., 2012). Their capacity to go through a similar somitic chondrogenesis program remains to be determined.

MATERIALS AND METHODS

Cells, factors and antibodies

Mouse E14 ESCs and green fluorescence protein (GFP)-Bry ESCs kindly provided by G. Keller (Toronto, Canada) were maintained on mouse embryonic fibroblast feeders as described previously (Nakayama et al., 2003, 1998). EBRTcH3 ESCs carrying IRES-Bsd in the *Oct3/4* locus (i.e. Blasticidin resistant) were maintained as described (Masui et al., 2005), except that the medium contained monothioglycerol (MTG, Sigma) in place of β-mercaptoethanol and was supplemented with 2 µg/ml Blasticidin S (InvivoGen) (hereafter EBR medium). The EBRβcatM cells were generated by inserting the Ctnnb1(S33Y)-Mer fusion gene (provided by T. Nakano, Osaka, Japan) i.e. the S33Y mutant β-catenin open reading frame fused with the FLAG-tag sequence at the N-terminus and the mutant estrogen receptor (Mer) sequence at the C-terminus, into the *Rosa26* locus via Cre recombinase-mediated site-directed recombination (supplementary material Fig. S1A). The EBRβcatM cells were maintained in EBR medium supplemented with 0.5 µg/ml puromycin (InvivoGen) and 1 µM tetracycline (Tet; Sigma-Aldrich). Expression of the Ctnnb1(S33Y)-Mer fusion gene was induced by removal or reduction of Tet, which can be monitored by the emergence of YFP (Masui et al., 2005). Two clones (EBRβcatM Cl24-5 and Cl3-8) were used for biological studies. The protein growth and differentiation factors and protein inhibitors, media and supplements, buffers and specialized tissue culture plates, and antibodies for FACS, were sourced as described (Nakayama et al., 2003, 1998, 2000; Tanaka et al., 2009).

Differentiation induction in a chemically defined medium

ESCs were subjected to the EB-forming culture in a CDM-based semisolid medium as described (Tanaka et al., 2009). In the case of EBRβcatM cells, the pre-culture medium included 1.5 µg/ml puromycin and 10 nM Tet, and the differentiation medium was supplemented with 3-4.5 µg/ml puromycin and 4 nM Tet. The high concentration of puromycin with a reduced concentration of Tet during EB formation was used to maximize the yield of viable YFP^+ progeny: i.e. viable progeny in which the *Rosa26* locus was not silenced. The differentiation medium was supplemented on day 2 of differentiation with Wnt3a (Tanaka et al., 2009) at 100 ng/ml, BMP4 (R&D Systems) at 2 ng/ml, Noggin (Noggin-Fc, R&D Systems) at 100-500 ng/ml, BIO, Acetoxime-BIO (AcBIO), 1-methyl BIO (MeBIO) (all from Calbiochem), and CHIR99021 (BioVision) at 5 µM, and/or LDN193189 (Stemgent) at 0.6 µM, unless otherwise stated. activin A (PeproTech) was added at 1-25 ng/ml, and SB431542 (Tocris Bioscience) at 1-3 µM. Activation of the expressed Ctnnb(S33Y)-Mer protein was achieved by addition on day 2 of 4-hydroxytamoxifen (OHT, Sigma) at 0.9 µM.

Flow cytometry on EB cells

Flow cytometric analysis of EB cells and fractionation by FACS were performed as described (Tanaka et al., 2009), except that the viable cells were gated using DAPI (Sigma), and the cell sorter used was Aria or Aria II (BD Biosciences). Since the $(Bry^+)Pdgfr\alpha^+$ cell fraction may contain endoderm, and since E-cadherin is a marker for endoderm (and ectoderm), E-cadherin (clone Decma1, Sigma) was added to the FACS strategy to ensure removal of the $E\text{-cadherin}^+$ endoderm within the $Pdgfr\alpha^+$ fraction.

Chondrogenesis cultures

Two-dimensional (2D)-micromass culture was initiated by spotting 1×10^5 cells in 5 µl to a well of a 24-well plate and maintained in the chondrogenesis medium supplemented with 40 ng/ml PDGF (PDGF-BB, R&D Systems) as described (Tanaka et al., 2009). When indicated, TGFβ (TGFβ3, R&D Systems) was added at 10 ng/ml on day 1. When the EBRβcatM clone-derived YFP^+P^+ EB cells were used, Tet was included at 1 µM to suppress the accumulation of Ctnnb(S33Y)-Mer protein. Furthermore, for induction of the somitic chondrogenesis program, the chondrogenic medium with PDGF was further supplemented with either 300 ng/ml Shh (SHH-N, R&D Systems) or 100 nM SAG1 (Calbiochem), together with either 0.3-0.6 µM LDN193189 or 100-200 ng/ml Nog, both of which were replaced on day 6 with 50 ng/ml BMP4 (R&D Systems). On day 12 to 20 of culture, the developed micromass was either fixed with 10% (v/v) buffered Zn-formalin (Z-Fix, American MasterTech), and stained with 1% (w/v) acid Alcian Blue (Sigma) pH 1, as described (Nakayama et al., 2003), or subjected to analyses of DNA, RNA and sulfated glycosaminoglycans (sGAGs). The stained micromasses were then treated with 400 µl/well of 4 M guanidine hydrochloride in Tris.HCl-EDTA pH 7.5 (Hoemann, 2004), and the absorbance of the extract was measured at 600 nm (OD600) using SpectraMax M2 (Molecular Devices) to determine the relative amount of bound sGAGs per micromass. The 3D pellet culture was carried out in the serum-free chondrogenesis medium with PDGF, as described (Tanaka et al., 2009). The concentrations of protein factors and timings of addition were the same as for the 2D micromass culture. Developed cartilage particles were fixed on days 21-30 of culture by Z-Fix, paraffin sectioned, and stained primarily with 0.1% (w/v) Toluidine Blue (Sigma).

Isolation and quantification of DNA, RNA and sulfated glycosaminoglycan from micromass

The micromass was lysed using the guanidine isothiocyanate buffer (RLT, Qiagen), insoluble materials separated, and then DNAs, RNAs and proteins were individually isolated using AllPrep DNA/RNA/Protein Mini Kit (Qiagen). The purified RNAs were used for real-time RT-PCR analyses. The isolated proteins and the insoluble materials were both subjected to papain digestion for 18-20 h at 60°C [125 µg/ml papain, 10 mM cysteine in sodium phosphate-EDTA pH 6.5 (all from Sigma)], and released sGAGs were quantified with 1,9-dimethyl methylene blue [DMMB (Sigma), 16 µg/ml in glycine-NaCl pH 3], as described (Hoemann, 2004), using bovine tracheal chondroitin-4-sulfate (Biocolor) as standard. The OD590-530 was measured with SpectraMax M2. The DNAs isolated with the AllPrep kit and DNAs present in the papain-digest of insoluble materials were quantified using Hoechst 33258 (Sigma, 0.2 µg/ml in Tris.HCl-EDTA-NaCl pH 7.5), as described (Hoemann, 2004). The fluorescence (emission 460 nm, excitation 360 nm) was measured with SpectraMax M2 or Infinite M1000 (Tecan). The amounts of sGAG and DNA from a soluble extract and the corresponding insoluble material were combined to obtain total sGAG and DNA per micromass (µg sGAG/mass, µg DNA/mass), and the amount of sGAG was normalized to the amount of corresponding DNA to determine the active chondrocyte population within each micromass (µg sGAG/µg DNA).

Development (2014) 141, 3848-3858 doi:10.1242/dev.105981

Subcutaneous transplantation of cartilage particles

One to three cartilaginous particles (2-3 mm 'wet' diameter), formed by 3D pellet culture for 21-28 days using freshly sorted Flk1^{-}Pdgfrα^{+} rostral paraxial mesoderm cells were wrapped in one 0.5 cm×1 cm Gelfoam (Pharmacia Upjohn) and transplanted to one or two sites under the dorsal skin of NSG mice. Ten to 12 weeks later, the cartilage/bone particles were harvested, fixed with Z-fix for 4 days, embedded in plastic, sectioned (5 μm), and stained with von Kossa counterstained with van Gieson, or with acid T-Blue [i.e. 0.1% (w/v) Toluidine Blue pH 3.7, 0.1% (w/v) urea (Sigma)]. The transplantation experiments were performed under the regulation of the IACUC for the University of Texas Health Science Center at Houston.

Real-time PCR for gene expression profiling

Total RNAs were purified with RNeasy Micro Kit or AllPrep RNA/DNA/Protein Mini Kit (Qiagen). Reverse transcription (RT) performed as described (Nakayama et al., 1998; Wang and Nakayama, 2009) was followed by the real-time quantitative PCR analysis using the ABI 7900 system (Applied Biosystems). All experiments were performed in duplicate or triplicate using either ABI SYBR Green Master mix and gene-specific primers, or ABI TaqMan Mix and TaqMan Gene Expression Assay (Applied Biosystems). The gene-specific oligonucleotide primers were purchased from Realtimeprimers.com or synthesized by IDT (supplementary material Table S1) (Tanaka et al., 2009). The eukaryotic translation elongation factor 1 alpha 1 (*Eef1a1*) gene was used as a reference gene, and the relative expression values were calculated as described (Wang and Nakayama, 2009). All RT-PCR results are presented as average relative expression levels with the s.d. shown as a thin vertical line. The *P*-value was determined by the Student's *t*-test using Excel or KaleidaGraph software.

Acknowledgements

We acknowledge T. Nakano for providing the Ctnnb1(S33Y)-Mer DNA constructs, Q. Yan for assistance in RT-PCR analyses, N. Matthias for transplantation, A. Hazen, D. Havilland and A. Fryga for cell sorting, S. Amra and M. Starbuck for histological sections and staining, and E. Zsigmond and A. Mitchell for proofreading.

Competing interests

The authors declare no competing financial interests.

Author contributions

J.Z., S.L., S.T., M.T., V.J.-J. and B.W. performed experiments and analysed data. H.N. constructed and provided the complete EBRTcH3 cell system. N.N. designed the research, performed additional experiments, analysed data and completed the preparation of the manuscript.

Funding

This work was supported partly by the Haemopoiesis Therapeutic Focus Fund [P017, P009 to N.N.] from the Australian Stem Cell Centre, by a Startup Fund (N.N.) from IMM UT Health, by the Rolanette and Berdon Lawrence Bone Disease Program of Texas Research Award (N.N.) and by the Innovative Research Grant of Arthritis Foundation (N.N.).

Supplementary material

Supplementary material available online at
http://dev.biologists.org/lookup/suppl/doi:10.1242/dev.105981/-/DC1

References

Akazawa, H., Komuro, I., Sugitani, Y., Yazaki, Y., Nagai, R. and Noda, T. (2000). Targeted disruption of the homeobox transcription factor Bapx1 results in lethal skeletal dysplasia with asplenia and gastroduodenal malformation. *Genes Cells* **5**, 499-513.

Chal, J. and Pourquié, O. (2009). Patterning and differentiation of the vertebrate spine. In *The Skeletal System* (ed. O. Pourquié), pp. 41-116. Cold Spring Harbor, NY: Cold Spring Harbor Laboratory Press.

Chen, J. K., Taipale, J., Young, K. E., Maiti, T. and Beachy, P. A. (2002). Small molecule modulation of Smoothened activity. *Proc. Natl. Acad. Sci. USA* **99**, 14071-14076.

Cohen, P. and Goedert, M. (2004). GSK3 inhibitors: development and therapeutic potential. *Nat. Rev. Drug Discov.* **3**, 479-487.

Craft, A. M., Ahmed, N., Rockel, J. S., Baht, G. S., Alman, B. A., Kandel, R. A., Grigoriadis, A. E. and Keller, G. M. (2013). Specification of chondrocytes and cartilage tissues from embryonic stem cells. *Development* **140**, 2597-2610.

Deutsch, U., Dressler, G. R. and Gruss, P. (1988). Pax 1, a member of a paired box homologous murine gene family, is expressed in segmented structures during development. *Cell* **53**, 617-625.

Dockter, J. L. (2000). Sclerotome induction and differentiation. *Curr. Top. Dev. Biol.* **48**, 77-127.

Fan, C.-M. and Tessier-Lavigne, M. (1994). Patterning of mammalian somites by surface ectoderm and notochord: evidence for sclerotome induction by a hedgehog homolog. *Cell* **79**, 1175-1186.

Fan, C.-M., Porter, J. A., Chiang, C., Chang, D. T., Beachy, P. A. and Tessier-Lavigne, M. (1995). Long-range sclerotome induction by sonic hedgehog: direct role of the amino-terminal cleavage product and modulation by the cyclic AMP signaling pathway. *Cell* **81**, 457-465.

Herbrand, H., Pabst, O., Hill, R. and Arnold, H.-H. (2002). Transcription factors Nkx3.1 and Nkx3.2 (Bapx1) play an overlapping role in sclerotomal development of the mouse. *Mech. Dev.* **117**, 217-224.

Hirsinger, E., Duprez, D., Jouve, C., Malapert, P., Cooke, J. and Pourquie, O. (1997). Noggin acts downstream of Wnt and Sonic Hedgehog to antagonize BMP4 in avian somite patterning. *Development* **124**, 4605-4614.

Hoch, R. V. and Soriano, P. (2003). Roles of PDGF in animal development. *Development* **130**, 4769-4784.

Hoemann, C. D. (2004). Molecular and biochemical assays of cartilage components. *In Cartilage and Osteoarthritis*, Vol. 2 (ed. F. de Ceuninck, M. Sabatini and P. Pastoureau), pp. 127-156. Totowa, NJ: Humana Press.

Hur, E.-M. and Zhou, F.-Q. (2010). GSK3 signalling in neural development. *Nat. Rev. Neurosci.* **11**, 539-551.

Inman, G. J., Nicolas, F. J., Callahan, J. F., Harling, J. D., Gaster, L. M., Reith, A. D., Laping, N. J. and Hill, C. S. (2002). SB-431542 is a potent and specific inhibitor of transforming growth factor-beta superfamily type I activin receptor-like kinase (ALK) receptors ALK4, ALK5, and ALK7. *Mol. Pharmacol.* **62**, 65-74.

Johnson, R. L., Laufer, E., Riddle, R. D. and Tabin, C. (1994). Ectopic expression of Sonic hedgehog alters dorsal-ventral patterning of somites. *Cell* **79**, 1165-1173.

Kempf, H., Ionescu, A., Udager, A. M. and Lassar, A. B. (2007). Prochondrogenic signals induce a competence for Runx2 to activate hypertrophic chondrocyte gene expression. *Dev. Dyn.* **236**, 1954-1962.

Koseki, H., Wallin, J., Wilting, J., Mizutani, Y., Kispert, A., Ebensperger, C., Herrmann, B. G., Christ, B. and Balling, R. (1993). A role for Pax-1 as a mediator of notochordal signals during the dorsoventral specification of vertebrae. *Development* **119**, 649-660.

Laping, N. J., Grygielko, E., Mathur, A., Butter, S., Bomberger, J., Tweed, C., Martin, W., Fornwald, J., Lehr, R., Harling, J. et al. (2002). Inhibition of transforming growth factor (TGF)-beta1-induced extracellular matrix with a novel inhibitor of the TGF-beta type I receptor kinase activity: SB-431542. *Mol. Pharmacol.* **62**, 58-64.

Lettice, L. A., Purdie, L. A., Carlson, G. J., Kilanowski, F., Dorin, J. and Hill, R. E. (1999). The mouse bagpipe gene controls development of axial skeleton, skull, and spleen. *Proc. Natl. Acad. Sci. USA* **96**, 9695-9700.

Marcelle, C., Stark, M. R. and Bronner-Fraser, M. (1997). Coordinate actions of BMPs, Wnts, Shh and noggin mediate patterning of the dorsal somite. *Development* **124**, 3955-3963.

Masui, S., Shimosato, D., Toyooka, Y., Yagi, R., Takahashi, K. and Niwa, H. (2005). An efficient system to establish multiple embryonic stem cell lines carrying an inducible expression unit. *Nucleic Acids Res.* **33**, e43.

McMahon, J. A., Takada, S., Zimmerman, L. B., Fan, C.-M., Harland, R. M. and McMahon, A. P. (1998). Noggin-mediated antagonism of BMP signaling is required for growth and patterning of the neural tube and somite. *Genes Dev.* **12**, 1438-1452.

Murry, C. E. and Keller, G. (2008). Differentiation of embryonic stem cells to clinically relevant populations: lessons from embryonic development. *Cell* **132**, 661-680.

Murtaugh, L. C., Chyung, J. H. and Lassar, A. B. (1999). Sonic hedgehog promotes somitic chondrogenesis by altering the cellular response to BMP signaling. *Genes Dev.* **13**, 225-237.

Nakayama, N. and Umeda, K. (2011). From pluripotent stem cells to lineage-specific chondrocytes: essential signalling and cellular intermediates. *In Embryonic Stem Cells: The Hormonal Regulation of Pluripotency and Embryogenesis* (ed. C. Atwood), pp. 621-648. Wien: INTECH.

Nakayama, N., Fang, I. and Elliott, G. (1998). Natural killer and B-lymphoid potential in CD34+ cells derived from embryonic stem cells differentiated in the presence of vascular endothelial growth factor. *Blood* **91**, 2283-2295.

Nakayama, N., Lee, J. and Chiu, L. (2000). Vascular endothelial growth factor synergistically enhances bone morphogenetic protein-4-dependent lymphohematopoietic cell generation from embryonic stem cells in vitro. *Blood* **95**, 2275-2283.

Nakayama, N., Duryea, D., Manoukian, R., Chow, G. and Han, C.-Y. E. (2003). Macroscopic cartilage formation with embryonic stem-cell-derived mesodermal progenitor cells. *J. Cell Sci.* **116**, 2015-2028.

Nishikawa, S.-I., Jakt, L. M. and Era, T. (2007). Embryonic stem-cell culture as a tool for developmental cell biology. *Nat. Rev. Mol. Cell Biol.* **8**, 502-507.

Oldershaw, R. A., Baxter, M. A., Lowe, E. T., Bates, N., Grady, L. M., Soncin, F., Brison, D. R., Hardingham, T. E. and Kimber, S. J. (2010). Directed

Development (2014) 141, 3848-3858 doi:10.1242/dev.105981

differentiation of human embryonic stem cells toward chondrocytes. *Nat. Biotechnol.* **28**, 1187-1194.

Provot, S., Kempf, H., Murtaugh, L. C., Chung, U.-I., Kim, D.-W., Chyung, J., Kronenberg, H. M. and Lassar, A. B. (2006). Nkx3.2/Bapx1 acts as a negative regulator of chondrocyte maturation. *Development* **133**, 651-662.

Rodrigo, I., Hill, R. E., Balling, R., Münsterberg, A. and Imai, K. (2003). Pax1 and Pax9 activate Bapx1 to induce chondrogenic differentiation in the sclerotome. *Development* **130**, 473-482.

Rodrigo, I., Bovolenta, P., Mankoo, B. S. and Imai, K. (2004). Meox homeodomain proteins are required for Bapx1 expression in the sclerotome and activate its transcription by direct binding to its promoter. *Mol. Cell. Biol.* **24**, 2757-2766.

Sato, N., Meijer, L., Skaltsounis, L., Greengard, P. and Brivanlou, A. H. (2004). Maintenance of pluripotency in human and mouse embryonic stem cells through activation of Wnt signaling by a pharmacological GSK-3-specific inhibitor. *Nat. Med.* **10**, 55-63.

Schier, A. F. (2009). Nodal morphogens. *Cold Spring Harb. Perspect. Biol.* **1**, a003459.

Tallquist, M. D., Weismann, K. E., Hellstroem, M. and Soriano, P. (2000). Early myotome specification regulates PDGFA expression and axial skeleton development. *Development* **127**, 5059-5070.

Tanaka, M., Jokubaitis, V., Wood, C., Wang, Y., Brouard, N., Pera, M., Hearn, M., Simmons, P. and Nakayama, N. (2009). BMP inhibition stimulates WNT-dependent generation of chondrogenic mesoderm from embryonic stem cells. *Stem Cell Res.* **3**, 126-141.

Tribioli, C. and Lufkin, T. (1999). The murine Bapx1 homeobox gene plays a critical role in embryonic development of the axial skeleton and spleen. *Development* **126**, 5699-5711.

Tribioli, C., Frasch, M. and Lufkin, T. (1997). Bapx1: an evolutionary conserved homologue of the Drosophila bagpipe homeobox gene is expressed in splanchnic mesoderm and the embryonic skeleton. *Mech. Dev.* **65**, 145-162.

Umeda, K., Zhao, J., Simmons, P., Stanley, E., Elefanty, A. and Nakayama, N. (2012). Human chondrogenic paraxial mesoderm, directed specification and prospective isolation from pluripotent stem cells. *Sci. Rep.* **2**, 455.

Wang, Y. and Nakayama, N. (2009). WNT and BMP signaling are both required for hematopoietic cell development from human ES cells. *Stem Cell Res.* **3**, 113-125.

Yamashita, S., Andoh, M., Ueno-Kudoh, H., Sato, T., Miyaki, S. and Asahara, H. (2009). Sox9 directly promotes Bapx1 gene expression to repress Runx2 in chondrocytes. *Exp. Cell Res.* **315**, 2231-2240.

Yu, P. B., Deng, D. Y., Lai, C. S., Hong, C. C., Cuny, G. D., Bouxsein, M. L., Hong, D. W., McManus, P. M., Katagiri, T., Sachidanandan, C. et al. (2008). BMP type I receptor inhibition reduces heterotopic [corrected] ossification. *Nat. Med.* **14**, 1363-1369.

Zeng, L., Kempf, H., Murtaugh, L. C., Sato, M. E. and Lassar, A. B. (2002). Shh establishes an Nkx3.2/Sox9 autoregulatory loop that is maintained by BMP signals to induce somitic chondrogenesis. *Genes Dev.* **16**, 1990-2005.

Fig. S1. Generation of EBRβcatM cells. (**A**) The *Rosa26* locus of EBRβcatM cells. The *Rosa26* locus of the parental EBRTcH3 cells was modified by Cre-dependent gene insertion so that the Ctnnb1(S33Y)-Mer gene was placed under the control of a Tet-repressible CMV promoter (CMV*). A low concentration of Tet will release the expression of the Ctnnb(S33Y)-Mer protein, and 4OHT will activate the protein. To construct such cell lines, the mouse Ctnnb1(S33Y)-Mer DNA fragment was amplified with PCR to introduce a Xho I site at the 5'-end and a Not I site at the 3'-end, and the amplified fragment was inserted into Xho I-Not I site of the pPthC donor plasmid (Masui et al., 2005). The resultant plasmid, pPthC-βcatM, contained Ctnnb1(S33Y)-Mer under the control of the Tet-repressive CMV promoter (CMV*-Ctnnb1(S33Y)-Mer) and a complete transcription unit for the expression of PacΔTK (PGK-PacΔTK-pA). EBRTcH3 ES cells carry a loxP-CMV*-Hph-loxP' cassette on the Rosa26 locus, and grow normally in EBR medium supplemented with 40 μg/ml Hygromycin B (Invitrogen) in the absence of Tet (EBR-Hyg medium) (Masui et al., 2005), which can be readily replaced by a donor cassette containing a different drug-resistant gene: e.g. CMV*-Ctnnb1(S33Y)-Mer with PGK- PacΔTk-pA via Cre-mediated site directed recombination (Masui et al., 2005). The expression vector for NLS-Cre recombinase, pHD2-Cre1, was kindly provided by Dr. Robert Ramsey (Melbourne, Australia). The EBRTcH3 cells were co-transfected with pPthC-βcatM and pHD2-Cre1 using Lipofectamine 2000 (Invitrogen, Carlsbad, CA), and were maintained for 2 days in the EBR medium supplemented with 1 μM Tet. Culture continued in the selection medium of EBR medium supplemented with1 μM Tet and 1.5 μg/ml of Puromycin (EBR-PurTet) for 9–11 days. The resulting colonies (approximately 20) were picked and individually maintained in a 24-well plate in the EBR-PurTet medium. Correct integrants were identified by

their ability to grow in EBR-PurTet medium but not in EBR-Hyg medium. (**B**) Copy-number of Ctnnb1 in EBRβcatM clones. Genomic DNA was purified from cultured EBRTcH3 cells and EBRβcatM clones (Cl3-2, 3-8, 21-3, 21-4, 24-5) using the Genomic DNA purification kit (Qiagen). Absolute Quantification PCR was done on the genomic DNA (primer pairs listed in Table S1) with the ABI 7500 system using the SYBR Green Master mix (Applied Biosystems). Triplicate experiments were performed for each DNA sample with each primer pair. Average Ct was calculated and ΔCt for Ctnnb1 exon-3 and Ctnnb1(S33Y)-Mer were calculated relative to the average Ct of Ctnnb1 intron-5 for each sample. The relative copy number of exon-3 in the isolated clones was calculated using the relative exon copy number of the parental EBRTcH3 cells as the base (i.e. 2 copies), and are plotted (B-catenin, red). All five clones show only 1 copy addition of Ctnnb1, suggesting that no non-specific integration had occurred in the isolated clones. The relative copy numbers of Ctnnb1(S33Y)-Mer in the clones were calculated using Cl3-2 as control (Mer, blue). (**C**) Expression of the Ctnnb(S33Y)-Mer protein in the EBRβcatM clones. EBRβcatM clones (Cl3-2, 3-8, 21-3, 21-4, 24-5) were propagated in EBR medium containing 0.5 μg/ml of Puromycin in the presence and absence of Tet for 3 days, confirmed by FACS to become YFP^+ in the absence of Tet, and subjected to Western blot analysis. Cells were lysed with 100 μl of Lysis Buffer: 50mM Tris-HCl pH8.0, 150mM NaCl, 1% (v/v) Triton X-100 (Sigma), 1x cOmplete Protease Inhibitor cocktail (Roche AS, Indianapolis, IN) at room temperature for 10 min, the extracts cleared, and the protein concentration determined (NanoDrop, Wilmington, DE). Twenty μg of each sample was subjected to SDS-PAGE, and blotted to Immobilon-FL PVDF membrane (Millipore, Billerica, MA). The membranes were blocked with Odyssey Blocking Buffer (Li-COR Biotech, Lincoln NE) for 1 h, then incubated for another 1 h in the presence of the primary antibodies anti-β-catenin (BD) and anti-β-tubulin

(Millipore, Temecula, CA). The blots were washed (x3) with PBST (0.05% [v/v] Tween-20 in PBS), and stained with secondary antibody IRDye700 (0.2 μg/ml) in Odyssey Blocking Buffer for 1 h. The blots were washed again with PBST, and scanned on an Odyssey Imager (Li-COR).

Fig. S2. Characterization of EBRβcatM Cl3-8 and Cl24-5 cells. (**A**) Experimental Scheme. EBRβcatM (Cl24-5 and Cl3-8) ES cells were differentiated by successive reduction in concentration of Tet and increase in concentration of Puromycin and by addition on day 2 of WNT3a (W), 500 ng/ml Noggin (N), BMP4 (B), and/or 4OHT (OHT). (**B**) EBRβcatM (Cl24-5) cells were differentiated with no factor (none, black triangle/line), W (pale pink), N (green), WN (blue), OHT (orange), or OHT+N (pink). EBs were harvested on the indicated days for RT-PCR. (**C**) Supplementary to Fig. 1B. RT-PCR analysis was also conducted using *Uncx* and *Hand2* primers. The preferential conditions for *Uncx* expression resemble those for *Meox1* expression, and the preferential conditions for *Hand2* expression are similar to those for *Foxf1a* expression. (**D**) (Left panel) EBRβcatM clones Cl24-5 and Cl3-8 were differentiated under conditions of OHT+N (brown), OHT+B (green) and OHT (blue) for 6 days. Then $YFP^+Flk1^-Pdgfr\alpha^+(YFP^+P^+)$ and $YFP^+Flk1^-Pdgfr\alpha^-(P^-)$ progeny were isolated by FACS from each condition, and were subjected to RT-PCR. The *Meox1* transcript was always enriched in the YFP^+P^+ progeny, but inclusion of BMP4 during differentiation (OHT+B) suppressed the *Meox1* level. (Right panel) EBRβcatM (Cl24-5) cells were differentiated with OHT+ N and various concentrations of Activin or SB431542 (SB). Then, RT-PCR for *Meox1* expression was performed. The dose-dependent effect of SB is plotted as "−μM" in the negative range. Activin at low concentrations (0 to 2 ng/ml) slightly enhanced the *Meox1* expression, but both SB and a higher concentration of Activin (>2 ng/ml) were strongly inhibitory. (**E**) EBRβcatM (Cl3-8) cells were differentiated

under OHT+N conditions for 6 days, and the $YFP^{+}P^{+}$ progeny were isolated and subjected to micromass culture in the presence of PDGF (P) and TGFβ (T) (Nakayama et al., 2003; Tanaka et al., 2009). The culture was fixed on day12, and stained with acid Alcian Blue. TGFβ enhancement of chondrogenesis (PT vs. P) was observed. Typical dark blue spots (signs of chondrogenesis) are highlighted with yellow arrowheads.

Fig. S3. (A-D) Feedforward system between WNT and BMP and between WNT and Nodal, but not between BMP and Nodal. (**A**) Experimental Scheme. E14, Bry-GFP, and EBRTcH3 ES cells were differentiated in the presence of no factor (none), WNT3a (W), BIO, MeBIO, 2 μg/ml Fzd8CRD-Fc (FZD), Noggin (N) with various concentrations of Activin added on day 2. (**B**) GSK3-inhibitor substitutes for Wnt3a on the *Bmp4* and *Nodal* induction during differentiation. Bry-GFP ES cells were differentiated in the presence of W (purple), BIO (green) and no factor (black) conditions. EBs were harvested on days 4, 5 and 6 and subjected to RT-PCR for *Bmp4* add *Nodal* expression. Compared to BIO, WNT3a induced *Bmp4* and *Nodal* more strongly and sooner than BIO. (**C**) Dose-dependent effects of Activin and WNT3a on *Bmp4* and *Nodal* gene expression during ES cell differentiation. E14 ES cells were differentiated for 5 days under conditions of no factor (black), N (green), W (purple), or WN (blue) with various concentrations of Activin or WNT3a. Note that Activin has no role in WNT3a-induced *Bmp4* expression and Noggin shows no effect on WNT3a-induced *Nodal* expression. (**D**) Nodal/Activin/TGFβ signal-dependent induction of mesoderm is achieved through endogenous WNT functions. EBRTcH3 (EBR) and Bry-GFP (BRY) ES cells were differentiated for 6 days using various concentrations of Activin in the presence of Noggin (N) with (blue) or without (brown, green) FZD. The *Meox1* expression induced by Activin + Noggin, the level of which

was much lower than that achieved by WNT3a + Noggin, was completely blocked by FZD in both cell lines, suggesting that the Nodal/Activin/TGFβ-induced mesoderm specification is mediated via endogenous WNT activity. (**E**) Titration of Noggin and GSK3 inhibitor. EBRTcH3 ES cells were differentiated in the presence of no factor (black triangle), WNT3a (W, purple), BIO (brown) and various concentrations of Noggin (Left two panels), or in the presence of various concentrations of BIO (brown) or MeBIO (black) alone (Right most panel). RNAs were extracted on day 6 and subjected to RT-PCR analysis. A concentration of 100 ng/ml is sufficient to induce *Meox1* and suppress *Foxf1a* expression. BIO-induction of *Meox1* depends on the "active" GSK3-inhibitor (BIO) but not the modified "inactive" version (MeBIO).

Fig. S4. Fine tuning of Nodal/Activin/TGFβ signaling for efficient generation of mesendoderm and mesoderm. (**A**) E14 ES cells were differentiated for 5 days in CDM in the presence of no factor (none, black), 500 ng/ml Noggin (N, red), 25 ng/ml Activin (A, green), or Activin + Noggin (A+N, blue) with various concentrations of WNT3a. RT-PCR was then performed using primers for *Tal1*, *Chrd*, and *Foxa2*. Note that Activin stimulates WNT3a-dependent *Tal1* (hemogenic angioblast marker) expression as well as (WNT3a + Noggin)-dependent *Chrd* and *Foxa2* (axial mesendoderm marker) expression. (**B**) E14 cells were differentiated in the presence of no factor (green), 500 ng/ml Noggin (N, purple), WNT3a (W, brown), and WNT3a + 500 ng/ml Noggin (WN, blue), together with various concentrations of Activin, and RT-PCR was performed using primers for the indicated genes. Note that high concentrations of Activin (>5 ng/ml) increased WNT3a-dependent *Tal1* expression and (WNT3a + Noggin)-dependent *Gsc* (mesendoderm marker) expression, but inhibited (WNT3a + Noggin)-dependent *Meox1* expression. (**C**) E14 ES cells were differentiated for 5 days in CDM in the

presence of 0 (A0) or 25 (A25) ng/ml Activin and 0 (W0), 5 (W5) or 50 (W50) ng/ml WNT3a. EBs were harvested for FACS analysis. Note that the genesis of the $Flk1^{+}Pdgfr\alpha^{-}$ hemogenic cell fraction (Tanaka et al., 2009) depends on high concentrations of Activin (A25) and WNT3a (W50). (**D**) Dose dependent effects of Nodal/Activin/TGFβ signaling on the GSK3-inhibitor induction of lateral plate mesoderm gene expression. EBRTcH3 ES cells were differentiated in the presence of no factor (black), BMP4 (B, purple), and BIO (brown), with various concentrations of SB and Activin, and RT-PCR was performed using primers for *Tal1* and *Foxf1a* (on day 6). Note that BIO-induced differentiation but not BMP-induced differentiation demonstrated the parabolic response to Nodal/Activin/TGFβ signaling. In conclusion, the BMP-dependent specification of lateral plate/extraembryonic mesoderm and hemoangiogenic mesoderm was not affected by the concentrations of SB and Activin tested. The WNT3a-induced specification of hemoangiogenic mesoderm and the (WNT3a + Noggin)-induced specification of axial mesendoderm were enhanced by Activin in a dose-dependent fashion. Thus, the optimal requirement of Nodal/Activin/TGFβ signaling for specification of subtypes of mesodermal and endodermal progeny is dependent on the inducer used.

Fig. S5. (**A**) Experimental Scheme. EBRTcH3 ES cells were differentiated for 6 days in the presence of WNT3a (W) and Noggin (N), or CHIR (C) and LDN (L) with or without SAG (S) added on day 4 (S4). (**B**) On average, the CL condition resulted in higher expression levels of *Meox1* than the WN condition in day 6 EBs (n=4). However, the difference was not statistically significant. P=0.145. (**C**) Supplementary for Fig. 3C. The results from RT-PCR using *Meox1* primers are provided. The E-cadherin^{-}Flk1^{-}Pdgfrα^{+} (P^{+}) progeny developed under CL and CLS4 were enriched in the *Meox1* transcript.

Fig. S6. (**A**) Experimental Scheme. EBRTcH3 ES cells were differentiated for 6 days in the presence of CHIR (C) and LDN (L) and various progeny were isolated by FACS and subjected to micromass culture for 12 days in the presence of various factors. (**B**) Time requirement of PSL treatment. The micromass culture initiated with E-cadherin$^-$Pdgfrα^+ cells under PDGF + SAG + LDN (PSL) was subjected to medium change (→) to PDGF + BMP (PB) on day3 and 6. Note: the standard 6-day treatment with LDN (PSL→PB) showed stronger chondrogenesis (slightly larger dark blue area) compared with the 3-day treatment (PSLday3→PB). (**C**) Supplementary for Fig. 4C. Effect of Noggin (N). The sorted E-cadherin$^-$Flk1$^-$Pdgfrα^+ progeny were subjected to micromass culture under PDGF + SAG (PS) or PDGF + SAG + Noggin (PSN) conditions, and the media were changed (→) to PB on day 6. Note: the 6-day treatment with Noggin enhanced chondrogenesis later, demonstrated by acid Alcian Blue stain. (**D**) Requirement of PSL conditions and E-cadherin$^-$Flk1$^-$Pdgfrα^+ (P$^+$) cells for successful chondrogenesis in micromass culture. Use of either Flk1$^-$Pdgfrα^- (P$^-$) cells, or the PDGF + LDN (PL) or PS conditions resulted in inefficient chondrogenesis as judged by Alcian Blue quantification as in Fig. 4D. Continuous presence of SAG is neither inhibitory nor stimulatory (PSL→PSB). * $P<0.05$. (**E**) Requirement of BMP4 from day 6 of micromass culture. The E-cadherin$^-$Flk1$^-$Pdgfrα^+ progeny were subjected to micromass culture under PDGF (P) or PSL conditions, and the media were changed (→) to P or PB on day 6. Note: Chondrogenesis is dependent on BMP signaling, when micromass culture was initiated under PSL conditions. (**F**) The E-cadherin$^-$Flk1$^-$Pdgfrα^+ progeny were subjected to micromass culture under P, PL, PS, or PSL conditions and the media were changed (→) to P, PB, or PSB on day 6. The cultures were subjected to Alcian Blue quantification as in Fig. 4D. * $P<0.05$. Note: The initial requirement of both SAG and LDN (PSL) and later requirement of

BMP (PB) for successful chondrogenesis was reproducibly shown. Continuous presence of SAG is again neither inhibitory nor stimulatory (PSL→PSB). (**G**) Supplementary to Fig. 4E. Quantification of sGAG and DNA. The total amounts of DNA and sGAG per micromass are displayed. * P<0.05

Fig. S7. Supplementary to Fig. 5C and Fig. 6B. (**A**) Experimental Scheme. (**B**) The same micromass cultures as performed for Fig. 5C were also subjected to RT-PCR with primers for the additional hypertrophic differentiation marker, *Alpl* (alkaline phosphatase gene). The *Bapx1* data are the same as shown in Fig. 5C but displayed without the PSL→PB data. (**C**,**D**) The micromass cultures performed for 14 days under PSN→PB (blue), PT→PTB (brown) and PT→PB (purple) conditions were periodically harvested for RT-PCR with primers for genes representing early chondrogenesis: *Bapx1* and *Sox9* (**C**) and for those representing chondrocytes: *Col2a1*, *Acan*, and *Col10a1* (**D**). Black triangle: freshly sorted cells. Note: (**D**) Continuous presence of TGFβ (after day 6) is neither inhibitory nor stimulatory for expressing (PT→PTB vs. PT→PB).

Fig. S8. (**A**) Experimental Scheme. (**B**) Supplementary to Fig. 5D. Quantification of sGAG and DNA. The micromass cultures performed under PT→PTB (brown), PSN→PB (blue), and PSL→PB (green) conditions were periodically harvested for total DNA and sGAG quantification. The amounts were normalized to one micromass to display μg sGAG/mass or μg DNA/mass. Black triangle: freshly sorted cells. Note: In support of the RNA results shown in Fig. 5C, LDN is a better alternative to Noggin for overall cellular growth (DNA) and cartilage matrix deposition (sGAG) during micromass culture. (**C**) Supplementary to Fig. 6B (upper panel). The levels of *Col10al* and *Col2a1* transcripts in the day 20 micromass developed under the indicated conditions have been used for the calculation. * P<0.05. (**D**,**E**) Supplementary to

Fig. 6C,D. Micromass cultures were initiated under the PSL→PB condition, which were converted to pellet culture on day 7, and continued till day 30. Some cartilage particles were fixed and stained with Toluidine Blue (T-Blue) (**D**) and some were transplanted into NSG mice for 12 weeks after which they were fixed, plastic embedded, and sectioned (**E**). The sections were subjected to von Kossa-van Gieson staining (left) and acid T-Blue staining (right).

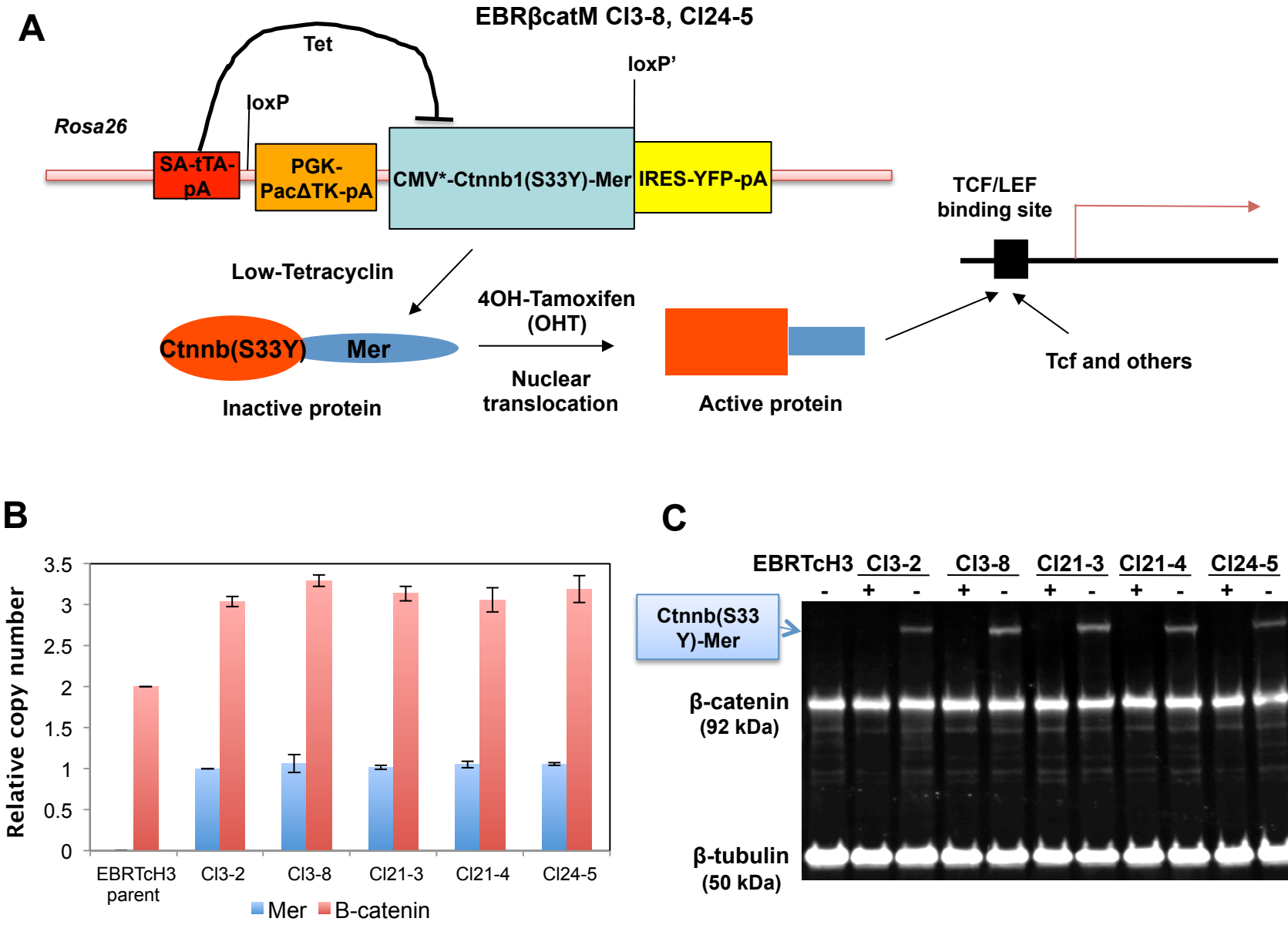
A
EBRβcatM Cl3-8, Cl24-5
Tet
loxP
loxP'
Rosa26
SA-tTA-pA
PGK-PacΔTK-pA
CMV*-Ctnnb1(S33Y)-Mer
IRES-YFP-pA
TCF/LEF binding site
Low-Tetracyclin
4OH-Tamoxifen (OHT)
Ctnnb(S33Y)
Mer
Inactive protein
Nuclear translocation
Active protein
Tcf and others
B
Relative copy number
3.5
3
2.5
2
1.5
1
0.5
0
EBRTcH3 parent
Cl3-2
Cl3-8
Cl21-3
Cl21-4
Cl24-5
Mer
B-catenin
C
EBRTcH3
Cl3-2
Cl3-8
Cl21-3
Cl21-4
Cl24-5
- + - + - + - + - + - Tet
Ctnnb(S33 Y)-Mer
β-catenin (92 kDa)
β-tubulin (50 kDa)

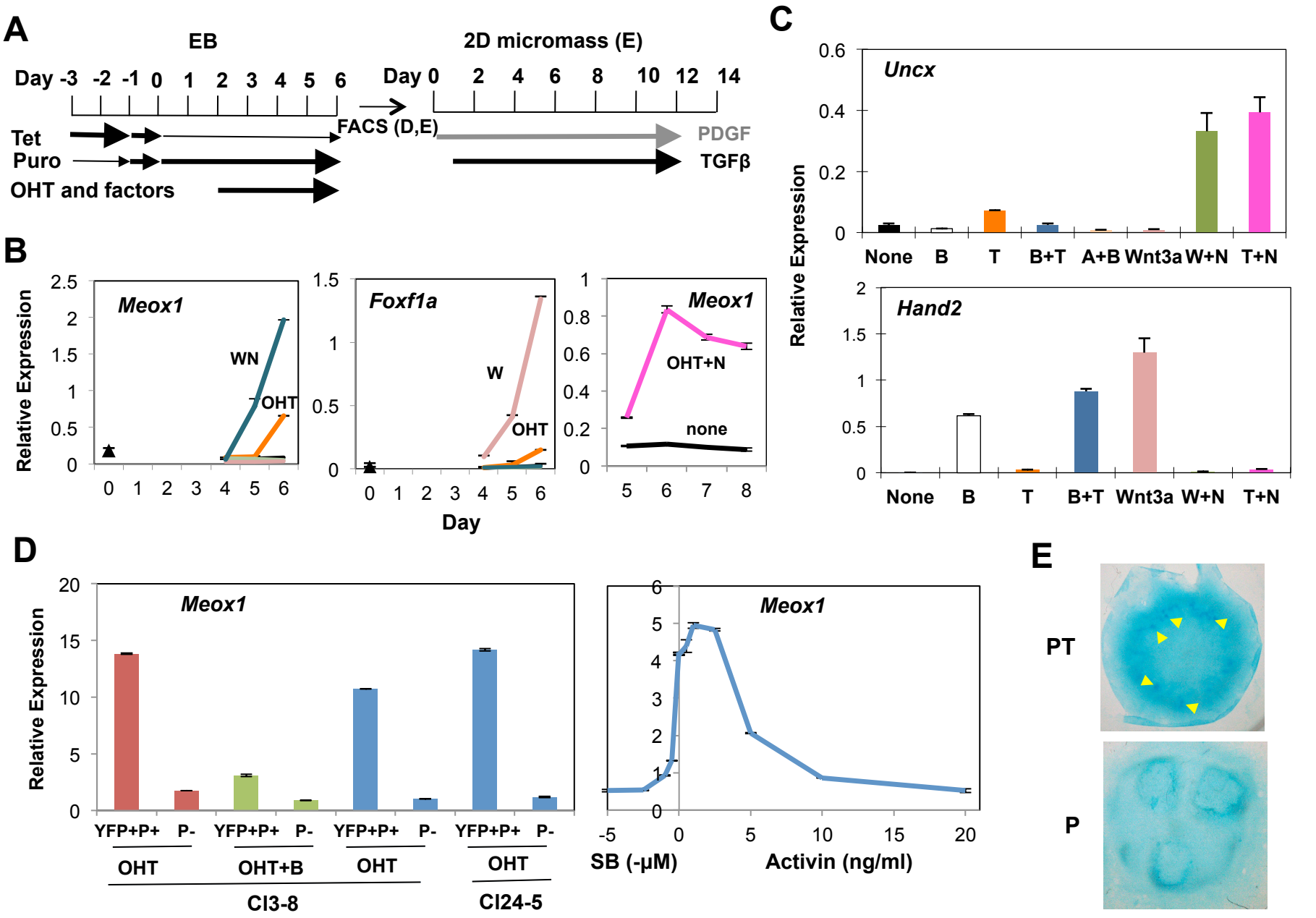
A
EB
2D micromass (E)
Day -3 -2 -1 0 1 2 3 4 5 6
Day 0 2 4 6 8 10 12 14
FACS (D,E)
Tet
Puro
OHT and factors
PDGF
TGFβ
B
Meox1
WN
OHT
Foxf1a
W
OHT
Meox1
OHT+N
none
Relative Expression
Day
C
Uncx
Hand2
Relative Expression
None B T B+T A+B Wnt3a W+N T+N
D
Meox1
Relative Expression
YFP+P+ P-
OHT
OHT+B
OHT
OHT
CI3-8
CI24-5
Meox1
SB (-μM)
Activin (ng/ml)
E
PT
P

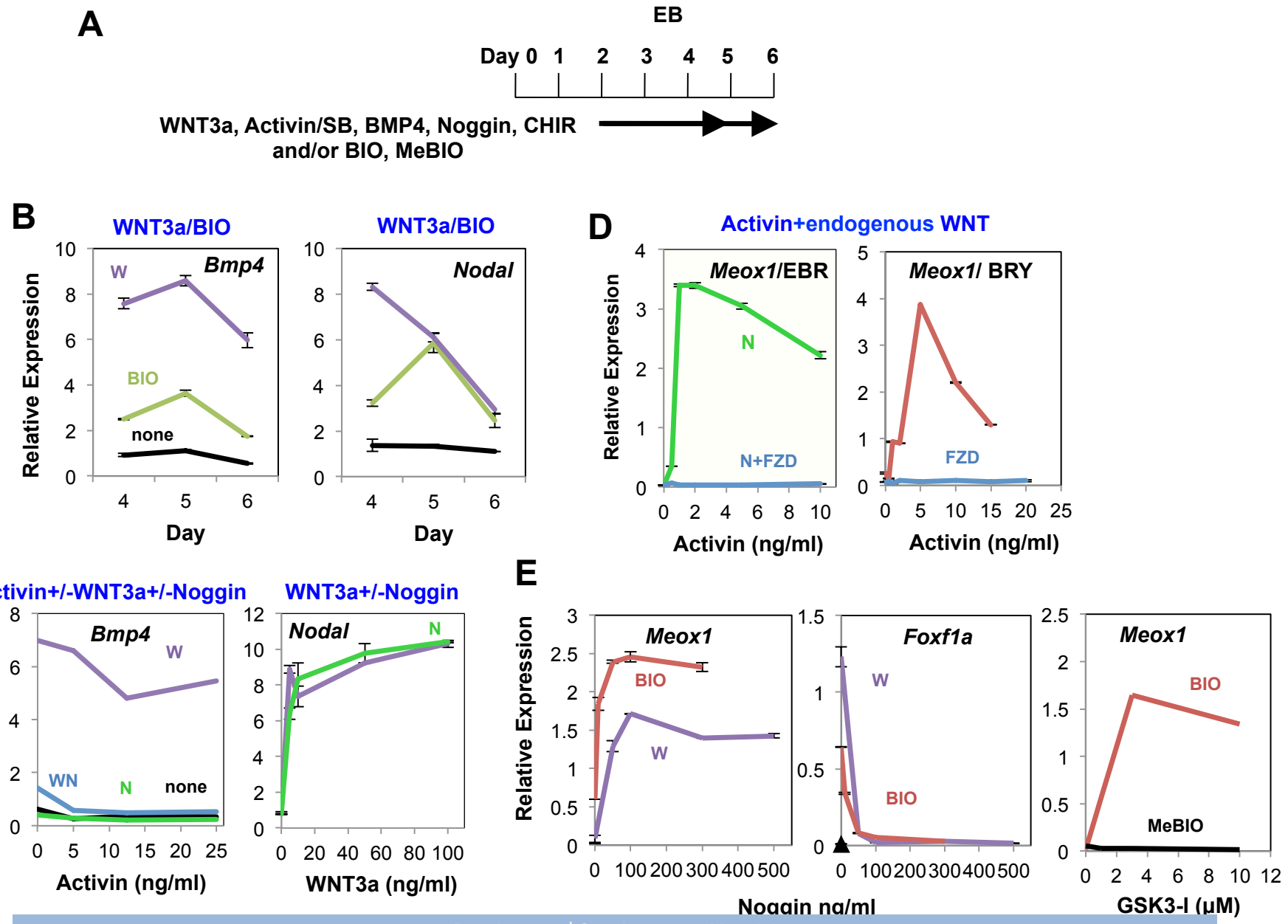
A
EB
Day 0 1 2 3 4 5 6
WNT3a, Activin/SB, BMP4, Noggin, CHIR and/or BIO, MeBIO
B
WNT3a/BIO
Bmp4
W
BIO
none
Relative Expression
Day
WNT3a/BIO
Nodal
Day
D
Activin+endogenous WNT
Meox1/EBR
N
N+FZD
Relative Expression
Activin (ng/ml)
Meox1/ BRY
FZD
Activin (ng/ml)
C
Activin+/-WNT3a+/-Noggin
Bmp4
W
WN
N
none
Relative Expression
Activin (ng/ml)
WNT3a+/-Noggin
Nodal
N
WNT3a (ng/ml)
E
Meox1
BIO
W
Relative Expression
Noggin ng/ml
Foxf1a
W
BIO
Meox1
BIO
MeBIO
GSK3-I (μM)

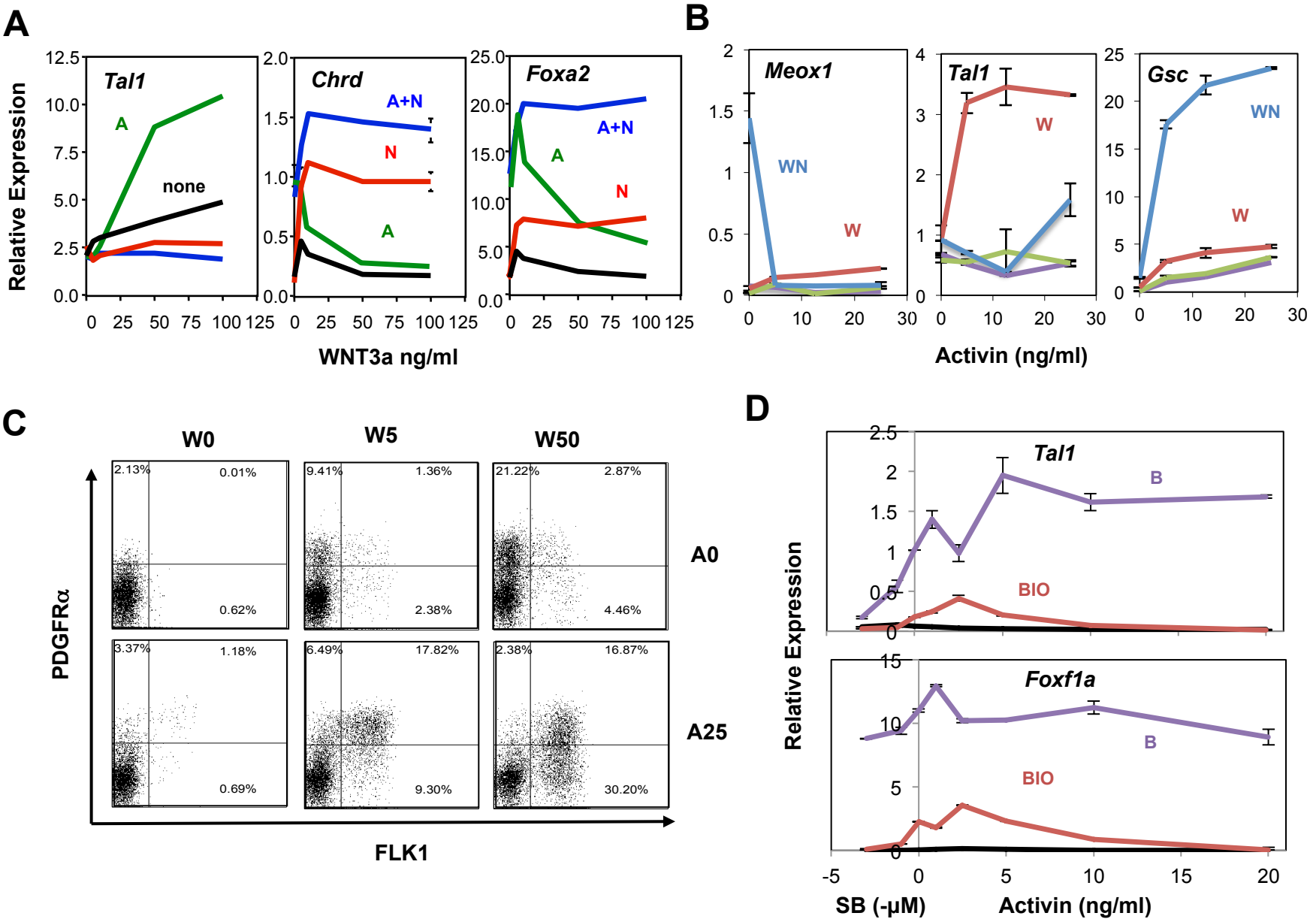
A
Relative Expression
Tal1
A
none
Chrd
A+N
N
A
Foxa2
A+N
A
N
WNT3a ng/ml
B
Meox1
WN
W
Tal1
W
Gsc
WN
W
Activin (ng/ml)
C
W0
W5
W50
2.13%
0.01%
0.62%
9.41%
1.36%
2.38%
21.22%
2.87%
4.46%
A0
3.37%
1.18%
0.69%
6.49%
17.82%
9.30%
2.38%
16.87%
30.20%
A25
PDGFRα
FLK1
D
Relative Expression
Tal1
B
BIO
Foxf1a
B
BIO
SB (-μM)
Activin (ng/ml)

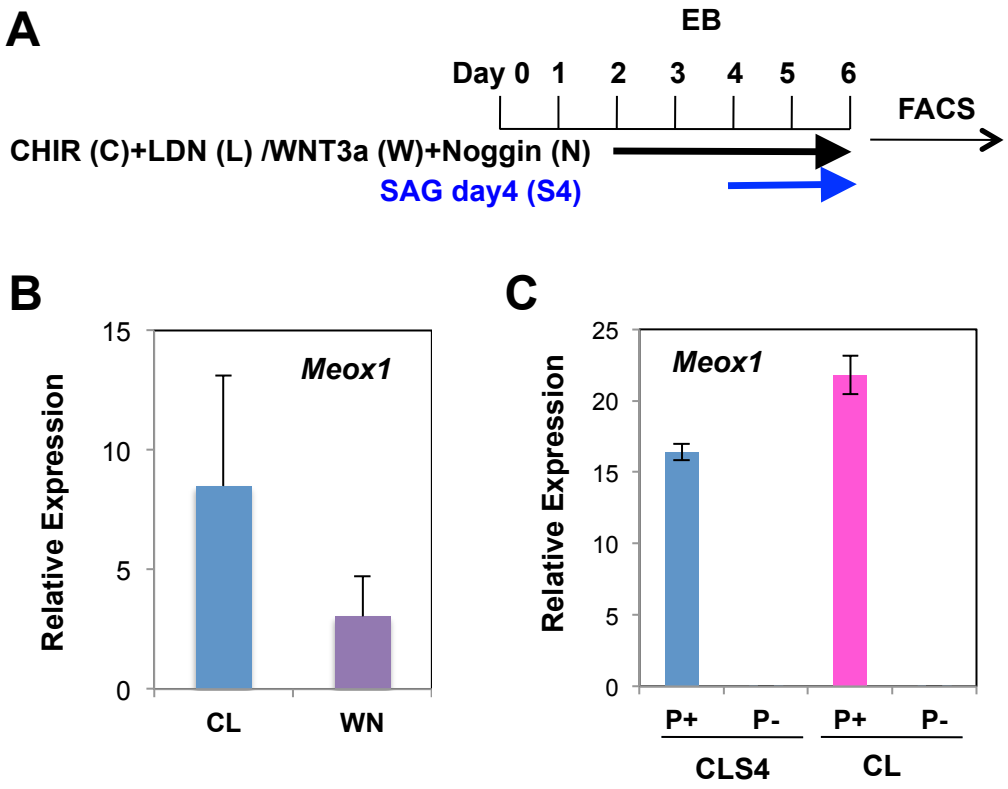
A
EB
Day 0 1 2 3 4 5 6
FACS
CHIR (C)+LDN (L) /WNT3a (W)+Noggin (N)
SAG day4 (S4)
B
Meox1
Relative Expression
15
10
5
0
CL
WN
C
Meox1
Relative Expression
25
20
15
10
5
0
P+
P-
P+
P-
CLS4
CL

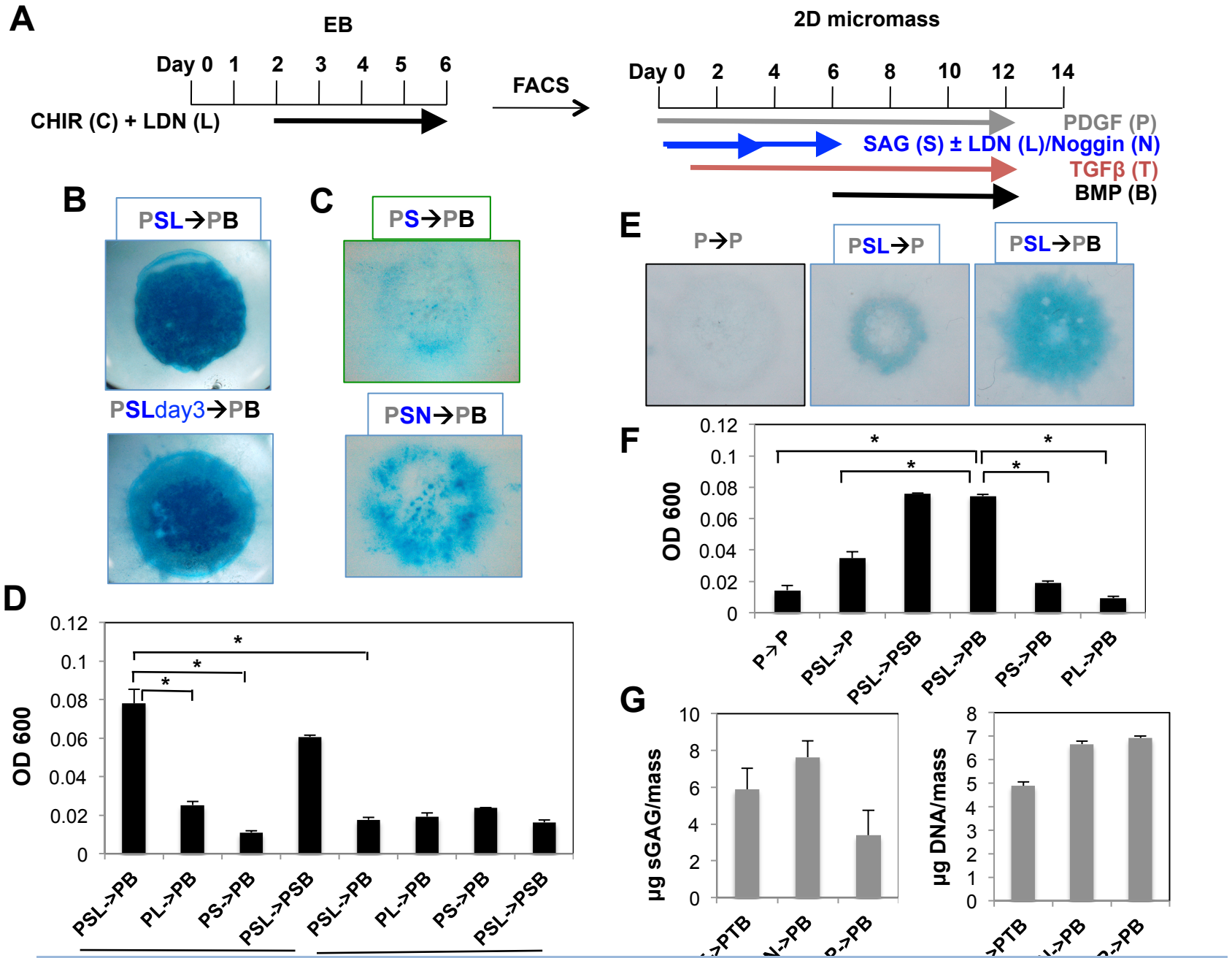
A
EB
Day 0 1 2 3 4 5 6
CHIR (C) + LDN (L)
FACS
2D micromass
Day 0 2 4 6 8 10 12 14
PDGF (P)
SAG (S) ± LDN (L)/Noggin (N)
TGFβ (T)
BMP (B)
B
PSL→PB
PSLday3→PB
C
PS→PB
PSN→PB
E
P→P
PSL→P
PSL→PB
F
OD 600
0.12
0.1
0.08
0.06
0.04
0.02
0
P→P
PSL→P
PSL→PSB
PSL→PB
PS→PB
PL→PB
D
OD 600
PSL->PB
PL->PB
PS->PB
PSL->PSB
PSL->PB
PL->PB
PS->PB
PSL->PSB
G
µg sGAG/mass
µg DNA/mass

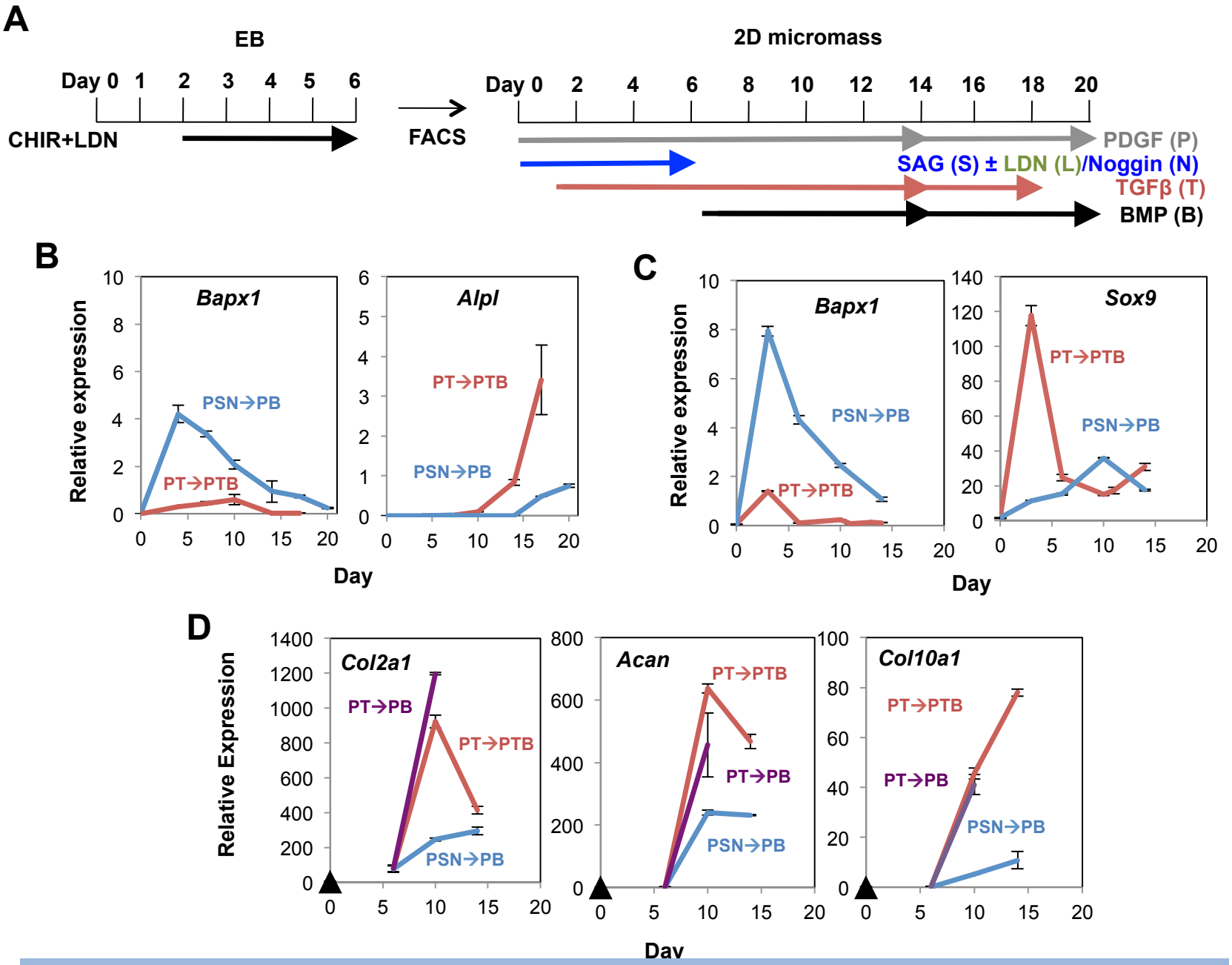
A
EB
Day 0 1 2 3 4 5 6
CHIR+LDN
FACS
2D micromass
Day 0 2 4 6 8 10 12 14 16 18 20
PDGF (P)
SAG (S) ± LDN (L)/Noggin (N)
TGFβ (T)
BMP (B)
B
Bapx1
Alpl
PSN→PB
PT→PTB
Relative expression
Day
C
Bapx1
Sox9
PSN→PB
PT→PTB
Relative expression
Day
D
Col2a1
Acan
Col10a1
PT→PB
PT→PTB
PSN→PB
Relative Expression
Day

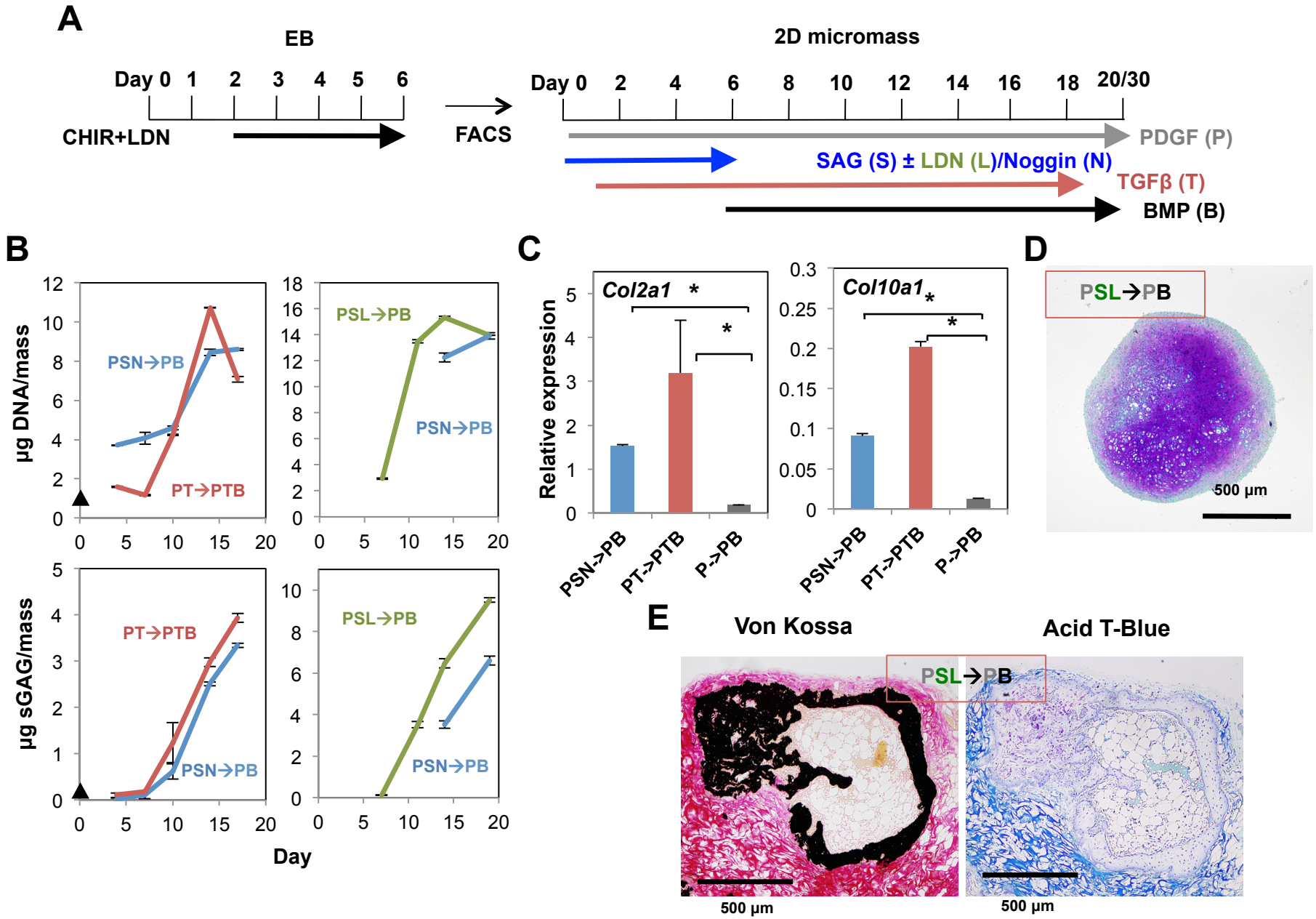
A
EB
Day 0 1 2 3 4 5 6
CHIR+LDN
FACS
2D micromass
Day 0 2 4 6 8 10 12 14 16 18 20/30
PDGF (P)
SAG (S) ± LDN (L)/Noggin (N)
TGFβ (T)
BMP (B)
B
µg DNA/mass
PSN→PB
PT→PTB
PSL→PB
PSN→PB
µg sGAG/mass
PT→PTB
PSN→PB
PSL→PB
PSN→PB
Day
C
Col2a1 *
Col10a1 *
Relative expression
PSN->PB
PT->PTB
P->PB
D
PSL→PB
500 µm
E
Von Kossa
Acid T-Blue
PSL→PB
500 µm
500 µm

Table S1. Primers

DNA PCR Primer	Location	Sequence 5'→3'
mCtnnB1-147F	Exon 3	GGG CAA CCC TGA GGA AGA A
mCtnnB1-210R	Exon 3	AAA GCC TTG CTC CCA TTC ATA A
mCtnnB1-intron5F	Intron 5	GTG GGC CAT GTC TTA AAG CAA
mCtnnB1-intron5R	Intron 5	TGC CTA GCT CAT TAA CTG CTC AAG
mCtnnB1-MerF	β-catenin-COOH	GCT GGC CTG GTT TGA TAC TGA
mCtnnB1-MerR	ER-NH_2	TCC TGA AGC ACC CAT TTC ATT

Gene	RT-PCR Primers	Sequence 5'→3'
Acan	(Realtimeprimers) F	TTC ACT GTA ACC CGT GGA CT
	(Realtimeprimers) R	TGG TCC TGT CTT CTT TCA GC
Col10a1	(Realtimeprimers) F	ATA GGC AGC AGC ATT ACG AC
	(Realtimeprimers) R	TAG GCG TGC CGT TCT TAT AC
Alpl	(Realtimeprimers) F	ACG AAT CTC AGG GTA CAC CA
	(Realtimeprimers) R	TGA GCT TTT GGA GTT TCA GG
Col2a1	F	GAA AAG AAA CAC ATC TGG TTT GGA
	R	TCT GGA CGT TAG CGG TGT TG
Bapx1	F	TGG GAC TTG ACA CAC CTA TCC A
	R	AGC GTC CCG AGG CTT GA
Sox9	F	TCA CAT CTC TCC TAA TGC TAT CTT CAA
	R	CGG CGG ACC CTG AGA TT
Nodal	F	CCT CCA GGC GCA AGA TGT
	R	CGC CCA TAC CAG ATC CTC TTC
Gsc	Taqman (Applied Biosystems)	
Foxf1a	Taqman (Applied Biosystems)	
Uncx	Taqman (Applied Biosystems)	

F: forward, R: reverse. Sequence information of other primers used will be found in (Tanaka et al., 2009).